Inorg. Chem. **2007**, *46*, 681–699

Accounting for the Differences in the Structures and Relative Energies of the Highly Homoatomic np_π–np_π ($n \geq 3$)-Bonded $S_2I_4^{2+}$, the Se–I π-Bonded $Se_2I_4^{2+}$, and Their Higher-Energy Isomers by AIM, MO, NBO, and VB Methodologies[||]

Scott Brownridge,[†] Margaret-Jane Crawford,[†] Hongbin Du,[†] Richard D. Harcourt,*[,‡] Carsten Knapp,[†] Risto S. Laitinen,[§] Jack Passmore,*[,†] J. Mikko Rautiainen,*[,†,£] Reijo J. Suontamo,[£] and Jussi Valkonen[£]

Departments of Chemistry, University of Jyväskylä, P.O. Box 35, FIN-40014, Finland, University of New Brunswick, Fredericton, New Brunswick, E3B 6E2, Canada, University of Melbourne, Victoria 3010, Australia, and University of Oulu, P.O. Box 3000, FIN-90014, Finland

Received August 11, 2006

The bonding in the highly homoatomic np_π–np_π ($n \geq 3$)-bonded $S_2I_4^{2+}$ (three σ + two π bonds), the Se–I π-bonded $Se_2I_4^{2+}$ (four σ + one π bonds), and their higher-energy isomers have been studied using modern DFT and ab initio calculations and theoretical analysis methods: atoms in molecules (AIM), molecular orbital (MO), natural bond orbital (NBO), and valence bond (VB) analyses, giving their relative energies, theoretical bond orders, and atomic charges. The aim of this work was to seek theory-based answers to four main questions: (1) Are the previously proposed simple π^*–π^* bonding models valid for $S_2I_4^{2+}$ and $Se_2I_4^{2+}$? (2) What accounts for the difference in the structures of $S_2I_4^{2+}$ and $Se_2I_4^{2+}$? (3) Why are the classically bonded isolobal P_2I_4 and As_2I_4 structures not adopted? (4) Is the high experimentally observed S–S bond order supported by theoretical bond orders, and how does it relate to high bond orders between other heavier main group elements? The AIM analysis confirmed the high bond orders and established that the weak bonds observed in $S_2I_4^{2+}$ and $Se_2I_4^{2+}$ are real and the bonding in these cations is covalent in nature. The full MO analysis confirmed that $S_2I_4^{2+}$ contains three σ and two π bonds, that the positive charge is essentially equally distributed over all atoms, that the bonding between S_2 and two I_2^+ units in $S_2I_4^{2+}$ is best described by two mutually perpendicular 4c2e π^*–π^* bonds, and that in $Se_2I_4^{2+}$, two SeI_2^+ moieties are joined by a 6c2e π^*–π^* bond, both in agreement with previously suggested models. The VB treatment provided a complementary approach to MO analysis and provided insight how the formation of the weak bonds affects the other bonds. The NBO analysis and the calculated AIM charges showed that the minimization of the electrostatic repulsion between EI_2^+ units (E = S, Se) and the delocalization of the positive charge are the main factors that explain why the nonclassical structures are favored for $S_2I_4^{2+}$ and $Se_2I_4^{2+}$. The difference in the structures of $S_2I_4^{2+}$ and $Se_2I_4^{2+}$ is related to the high strength of the S–S π bond compared to the weak S–I σ bond and the additional stabilization from increased delocalization of positive charge in the structure of $S_2I_4^{2+}$ compared to the structure of $Se_2I_4^{2+}$. The investigation of the $E_2X_4^{2+}$ series (E = S, Se, Te; X = Cl, Br, I) revealed that only $S_2I_4^{2+}$ adopts the highly np_π–np_π ($n \geq 3$)-bonded structure, while all other dications favor the π-bonded $Se_2I_4^{2+}$ structure. Theoretical bond order calculations for $S_2I_4^{2+}$ confirm the previously presented experimentally based bond orders for S–S (2.1–2.3) and I–I (1.3–1.5) bonds. The S–S bond is determined to have the highest reported S–S bond order in an isolated compound and has a bond order that is either similar to or slightly less than the Si–Si bond order in the proposed triply bonded $[(Me_3Si)_2CH]_2(^iPr)SiSi{\equiv}SiSi(^iPr)[CH(SiMe_3)_2]_2$ depending on the definition of bond orders used.

1. Introduction

All π bonds are weaker than the corresponding σ bonds, with few exceptions, e.g., N−N, O−O, and combinations thereof, and the relative difference increases as the groups are descended (see Table 1).[1] Multiple bonds between carbon atoms are thermodynamically unstable relative to singly bonded polymeric alternatives but can be kinetically stable.

The first isolated doubly bonded molecule of the heavier elements of Groups 13, 14, and 15 was tetramesityldisilene, prepared in 1981.[3] The Si═Si double bond is kinetically and thermodynamically stabilized from polymerization by bulky

[||] This paper is dedicated to Professor Neil Bartlett on the occasion of his 75th birthday.

* To whom correspondence should be addressed. E-mail: passmore@unb.ca (J.P., Overall concepts, questions, and solutions); r.harcourt@unimelb.edu.au (R.D.H., Valence Bond Section); mirauta@jyu.fi (J.M.R., Theoretical calculations). Phone: 1 (506) 4534821 (J.P.); 358 (14) 2602617 (J.M.R.). Fax: 1 (506) 4534981 (J.P.); 61 (3) 93475180 (R.D.H.); 358 (14) 2602501 (J.M.R.).

[†] University of New Brunswick.
[‡] University of Melbourne.
[§] University of Oulu.
[£] University of Jyväskylä.

10.1021/ic061523w CCC: $37.00
Published on Web 01/10/2007

Table 1. Selected σ and π Bond Strengths [kJ/mol] of Main Group Elements[a]

	13	14[b]	15[c]	16[b]	17
	B	C	N	O	F
σ	293 ± 21	346	167	142	155
π		256 ± 21	387 ± 13	352 ± 1	
	Al	Si	P	S	Cl
σ	133[d]	222	201	226	240
π		103[d]	140 ± 8	199 ± 7	
	Ga	Ge	As	Se	Br
σ	113 ± 17	188	146	172	190
π		84 ± 21	117 ± 21	100	
			Sb	Te	I
σ			121	126	149
π			87 ± 7	92 ± 8	

[a] See ref 1. [b] π-bond energy is the difference between double and single bonds. [c] π-bond energy is half of the difference between triple and single bonds. [d] See ref 2.

ligands.[4] Since then, an impressive array of related examples of Group 13, 14, and 15 multiply bonded species have been characterized,[5−7] including the recently prepared proposed triply bonded $[(Me_3Si)_2CH]_2(^iPr)SiSi{\equiv}SiSi(^iPr)[CH(SiMe_3)_2]_2$.[8] The nonplanar geometries of the R_2EER_2 and nonlinear geometries of REER (E = Si, Ge, Sn, P, As, Sb, Bi, R = bulky group) and $[RGaGaR]^{2-}$ have led to extensive discussion about the actual bonding and the EE bond order in these molecules.[6−9]

(1) Huheey, J. E. *Inorganic Chemistry: Principles of Structure and Reactivity*, 2nd ed.; Harper and Row: New York, 1978.
(2) Lide, D. R., Ed. *CRC Handbook of Chemistry and Physics, Internet version 2005*; http://www.hbcpnetbase.com; CRC Press: Boca Raton, FL, 2005
(3) West, R.; Fink, M. J.; Michl, J. *Science* **1981**, *214*, 1343.
(4) (a) Bulky groups weaken the σ bonds in the strained polymer, as well as kinetically hindering polymerization. (b) Burford, N.; Clyburne, J. A. C.; Chan, M. S. W. *Inorg. Chem.* **1997**, *36*, 3204.
(5) (a) Cowley, A. H. *Polyhedron* **1984**, *3*, 389. (b) Cowley, A. H. *Acc. Chem. Res.* **1984**, *17*, 386. (c) West, R.; Stone, F. G. A.; Eds. *Multiply Bonded Main Group Metals and Metalloids*; Academic Press: San Diego, 1996. (d) Power, P. P. *J. Chem. Soc., Dalton Trans*. **1998**, 2939. (e) Power, P. P. *Chem. Rev*. **1999**, *99*, 3463. (f) Robinson, G. H. *Adv. Organomet. Chem*. **2001**, *47*, 283. (g) West, R. *Polyhedron* **2002**, *21*, 467. (h) Weidenbruch, M. *Organometallics* **2003**, *22*, 4348. (i) Weidenbruch, M. *Angew. Chem*. **2003**, *115*, 2322; *Angew. Chem., Int. Ed*. **2003**, *42*, 2224. (j) Power, P. P. *Chem. Commun*. **2003**, 2101.
(6) (a) Xie, Y.; Schaefer, H. F., III; Robinson, G. H. *Chem. Phys. Lett*. **2000**, *317*, 174. (b) Xie, Y.; Grev, R. S.; Gu, J.; Schaefer, H. F., III; Schleyer, P. v. R.; Su, J.; Li, X.-W.; Robinson, G. H. *J. Am. Chem. Soc*. **1998**, *120*, 3773. (c) Robinson, G. H. *Acc. Chem. Res*. **1999**, *32*, 773. (d) Weidenbruch, M. *Angew. Chem.* **2005**, 117, 518; *Angew. Chem., Int. Ed.* **2005**, *44*, 514.
(7) (a) Wiberg, N.; Niedermayer, W.; Fischer, G.; Nöth, H.; Suter, M. *Eur. J. Inorg. Chem*. **2002**, 1066. (b) Takagi, N.; Nagase, S. *Chem. Lett*. **2001**, 966. (c) Takagi, N.; Nagase, S. *Eur. J. Inorg. Chem*. **2002**, 2775. (d) Wiberg, N.; Vasisht, S. K.; Fischer, G.; Mayer P. Z. *Anorg. Allg. Chem*. **2004**, *630*, 1823.
(8) (a) Sekiguchi, A.; Kinjo, R.; Ichinohe, M. *Science* **2004**, 305, 1755. (b) West, R. *Science* **2004**, *305*, 1724.
(9) (a) Malcom, N. O. J.; Gillespie, R. J.; Popelier, P. L. A. *Dalton Trans.* **2002**, 3333. (b) Bridgeman, A. J.; Ireland, L. R. *Polyhedron* **2001**, *20*, 2841. (c) Chesnut, D. B. *Heteroat. Chem.* **2002**, *13*, 53. (d) Pignedoli, C. A.; Curioni, A.; Andreoni, W. *ChemPhysChem* **2005**, *6*, 1795. (e) Frenking, G.; Krapp, A.; Nagase, S.; Takagi, N.; Sekiguchi, A. *ChemPhysChem* **2006**, *7*, 799. (f) Pignedoli, C. A.; Curioni, A.; Andreoni, W. *ChemPhysChem* **2006**, *7*, 801 (g) Chesnut, D. B. *Heteroat. Chem*. **2003**, *14*, 175. (h) Molina, J.; Dobado, J.A.; Heard, G. L.; Bader, R. F. W.; Sundberg, M. R. *Theor. Chem. Acc.* **2001**, *105*, 365. (i) Grützmacher, H.; Fässler, T. F. *Chem.-Eur. J.* **2000**, *6*, 2317. (j) Landis, C. R.; Weinhold, F. *J. Am. Chem. Soc*. **2006**, *128*, 7335. (k) Lein, M.; Krapp, A.; Frenking, G. *J. Am. Chem. Soc*. **2005**, *127*, 6290. (l) Jung, Y.; Brynda, M.; Power, P. P.; Head-Gordon, M. *J. Am. Chem. Soc*. **2006**, *128*, 7185.

Table 2. Selected Examples of Compounds and Cations Containing Element−Element Multiple Bonds (BO > 1) of Group 16 and 17 Elements

	E−E bond length [Å]			
	single bonds	multiple bonds	year of first structure determination	ref
MeSSMe(g)	2.022(±0.003)		1971[b]	10a
$Ph_3PNSNS{=}S$(s)		1.908(2)	1980[c]	10b
S_7I^+(s)[a]		1.906(5)	1976[c]	10c,d
$C_6H_3(t\text{Bu})_2(Me)NS{=}S$		1.898(2)	1979[c]	10e
$S{=}S{=}O$(g)		1.882	1959[d]	10f
$S{=}SF_2$(g)		1.856(2)	1989[b,d]	10g,11
$(S_2I_4)[AsF_6]_2$		1.828(11)	1980[c]	12
MeSeSeMe(g)	2.326(±0.004)		1971[b]	10h
Se_4^{2+}(s)		2.296(1)	1968[c]	10i−k
$[W(CO)_5(Se{=}Se)]^+$(s)		2.213(2)	1986[c]	10l
MeTeTeMe(g)	2.686(±0.003)		1990[b]	10m
Te_4^{2+}(s)		2.660(2)	1972[c]	10i,j
Cl_2(g)	1.986(±0.003)		1963[b]	10n
$Cl_2O_2^+$(s)		1.909(1)	1999[c]	10o
Br_2(g)	2.281		1974[e]	10p
Br_2^+(s)		2.15(1)	1971[c]	10i
I_2(g)	2.666		1974[e]	10p
I_2^+(s)		2.557(4)	1969[c]	10q, 11

[a] A figure of the crystal structure including bond lengths is given in the Supporting Information. [b] Gas-phase electron diffraction. [c] X-ray crystal structure. [d] Microwave spectroscopy. [e] Raman spectroscopy.

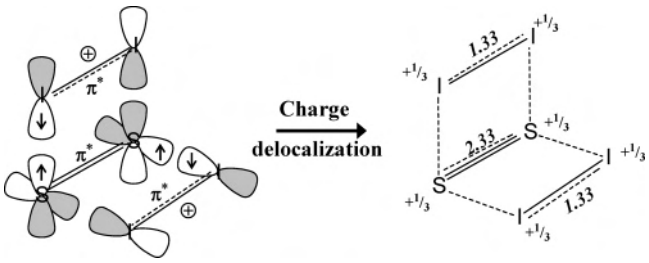

Figure 1. Bonding of $S_2I_4^{2+}$ is described as S_2 interacting with two I_2^+ in two mutually perpendicular planes via the unpaired electrons donating into π^* orbitals of each I_2^+. The positive charge delocalization results in equal charge distribution over all atoms and S−S and I−I bond orders of 2.33 and 1.33, respectively.

The weakening of $np_\pi-np_\pi$ bonds compared to σ bonds is less pronounced for the heavier elements of Groups 16 and 17 than for Groups 13−15 (see Table 1). Thus numerous examples of $2p_\pi-3p_\pi$ and even $3p_\pi-3p_\pi$ homoatomic multiple bonds of Group 16 and 17 heavier elements, all without any steric protection at all, have been known for some time (see Table 2). However, discussions of possible candidates for highly multiply bonded species of heavier main group elements, with a few exceptions,[5e,11] have not included the well-established examples from Groups 16 and 17.

$S_2I_4^{2+}$ was first prepared by Passmore et al. as an AsF_6^- salt in 1980,[12] and the bonding of $S_2I_4^{2+}$ was discussed using simple bonding models. The bonding in $S_2I_4^{2+}$ (see Figure 1) was described using frontier molecular orbital (FMO) theory, as arising from the interaction of the unpaired electrons in S_2 and two I_2^+ via two mutually perpendicular four center two electron, 4c2e, $\pi^*-\pi^*$ bonds[13] with subsequent positive charge delocalization over the entire molecule as a consequence of the near equality of the ionization energies (IE) of I_2 (9.39 eV) and S_2 (9.40 eV), leading to three σ and two delocalized π bonds.[12,14] In 1992, the

structure of the SbF_6^- salt was reported and the previously proposed qualitative model was supported by HF/STO-3G calculations using $O_2Cl_4^{2+}$ as a model system.[15] The bonding in $S_2I_4^{2+}$ has also been studied using valence bond theory[16,17] and discussed in several review articles.[5e,18] In 2005, we presented experimental evidence based on bond distances, vibrational frequencies, and force constants, that $S_2I_4^{2+}$ in $(S_2I_4)[MF_6]_2$ (M = As, Sb) was the most highly multiply bonded species in Groups 16 and 17 with an S−S bond order of 2.2−2.4 and an I−I bond order of 1.3−1.4.[11] This S−S bond order is higher than that of any of the formally doubly bonded Group 13, 14, and 15 molecules and higher than in any isolated Group 16 or 17 molecules. The S−S bond order, based on the experimental evidence,[11] is comparable to the theoretical Si−Si bond order calculated for $[(Me_3Si)_2CH]_2$-(^{i}Pr)SiSi≡SiSi(^{i}Pr)$[CH(SiMe_3)_2]_2$.[9d]

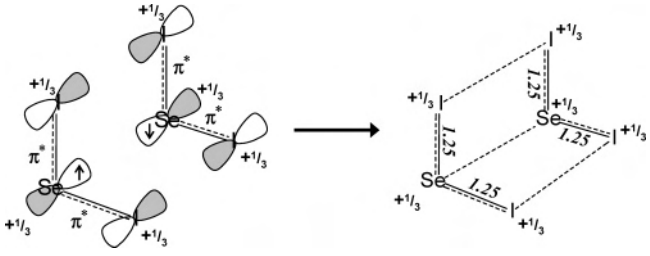

Figure 2. Bonding of $Se_2I_4^{2+}$ is described as a weak dimer of two SeI_2^+ resulting from the interaction of two π* SeI_2^+ SOMOs.

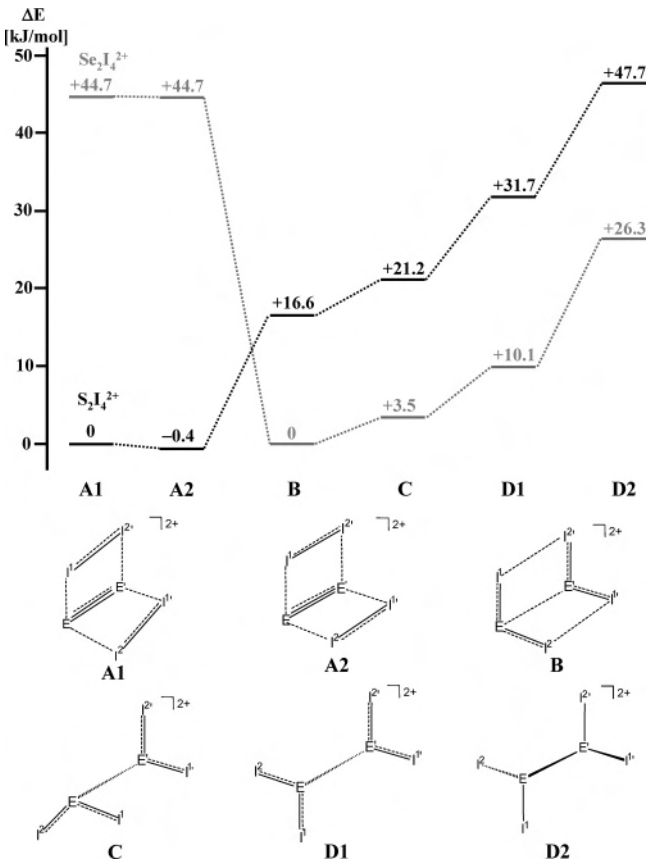

Figure 3. Calculated relative CCSD(T)/SDB-cc-pVTZ//PBE0/SDB-cc-pVTZ energies of different isomers of $S_2I_4^{2+}$ (black lines) and $Se_2I_4^{2+}$ (gray lines).

$S_2I_4^{2+}$ does not adopt the expected classically σ-bonded trans structure of the isoelectronic P_2I_4 molecule (**D2** in Figure 3).[19] Instead, the experimental structures of $S_2I_4^{2+}$ in Figure 3 (**A1** (C_2 symmetry as in the AsF_6^- salt) and **A2** (C_{2v} symmetry as in the SbF_6^- salt)) are composed of two planar quadrilateral $S_2I_2^+$ units with a common S−S bond and interplanar angle of nearly 90° resulting in a slightly distorted triangular prism. Both experimental structures of $S_2I_4^{2+}$ have very short S−S and I−I but very long S−I bonds and imply the presence of three σ and two delocalized π bonds. This is in contrast to the preference of third row elements to maximize σ-bond formation. It has been proposed that $S_2I_4^{2+}$ and related species adopt π-bonded

(10) (a) Beagley, B.; McAloon, K. T. *Trans. Faraday Soc*. **1971**, *67*, 3216. (b) Chivers, T.; Oakley, R. T.; Cordes, A. W.; Swepston P. *J. Chem. Soc., Chem. Commun*. **1980**, 35. (c) Passmore, J.; Taylor, P.; Whidden, T. K.; White, P. *J. Chem. Soc., Chem. Comm*. **1976**, *17*, 689. (d) Passmore, J.; Sutherland, G.; Taylor, P.; Whidden, T. K.; White, P. S. *Inorg. Chem*. **1981**, *20*, 3839. (e) Iwasaki, F. *Acta Crystallogr*. **1979**, *B35*, 2099. (f) Tiemann, E.; Hoeft, J.; Lovas, F. J.; Johnson, D. R. *J. Chem. Phys*. **1974**, *60*, 5000. (g) Marsden, C. J.; Oberhammer, H.; Lösking, O.; Willner, H. *J. Mol. Struct*. **1989**, 193, 233. (h) D'Antonio, P.; George, C.; Lowrey, A. H.; Karle, J. *J. Chem. Phys*. **1971**, *55*, 1071. (i) Brownridge, S.; Krossing, I.; Passmore, J.; Jenkins, H. D. B.; Roobottom, H. K. *Coord. Chem. Rev*. **2000**, *197*, 397 and references therein. (j) Beck, J. *Coord. Chem. Rev*. **1997**, *163*, 55 and references therein. (k) Beck, J.; Hilbert, T. Z. *Anorg. Allg. Chem*. **2000**, *626*, 837. (l) Collins, M. J.; Gillespie, R. J.; Kolis, J. W.; Sawyer, J. F. *Inorg. Chem*. **1986**, *25*, 2057. (m) Haaland, A.; Hammel, A.; Thomassen, H.; Volden H. V.; Singh, H. B.; Khanna, P. K. *Z. Naturforsch*. **1990**, *B45*, 1143. (n) Shibata, S. *J. Phys. Chem*. **1963**, *67*, 2256. (o) Drews, T.; Koch, W.; Seppelt, K. *J. Am. Chem. Soc*. **1999**, *121*, 4379. (p) Huber, K.P.; Herzberg, G. Constants of Diatomic Molecules (data prepared by J.W. Gallagher and R.D. Johnson, III). In *NIST Chemistry WebBook*; Linstrom, P.J., Mallard, W.G., Eds.; NIST Standard Reference Database Number 69; National Institute of Standards and Technology: Gaithersburg, MD, 2006. http://webbook.nist.gov. (q) Davies, C. G.; Gillespie, R. J.; Ireland, P. R.; Sowa, J. M. *Can. J. Chem*. **1974**, *52*, 2048.

(11) Brownridge, S.; Cameron, T. S.; Du, H.; Knapp, C.; Köppe, R.; Passmore, J.; Rautiainen, J. M.; Schnöckel, H. *Inorg. Chem*. **2005**, *44*, 1660 and references therein.

(12) Passmore, J.; Sutherland, G. W.; Whidden, T. K.; White, P. S. *J. Chem. Soc., Chem. Commun*. **1980**, 289.

(13) The 4c2e π*−π* bonds can also be regarded as 4c6e bonds and 6c2e π*−π* bonds as 6c10e bonds, depending on whether the π electrons on lower bonding and antibonding orbitals are expected to take part in the effective bonding or cancel each other out.

(14) (a) Rosenstock, H. M.; Draxl, K.; Steiner, B. W.; Herron, J. T. J. *Phys. Chem. Ref. Data* **1977**, *6* (Suppl. 1). (b) Wagman, D. D.; Evans, W. H.; Parker, V. B.; Schumm, R. H.; Halow, J.; Bailey, S. M.; Chruney, K. L.; Nuttall, R. L. *J. Phys. Chem. Ref. Data* **1982**, *11* (Suppl. 2). (c) Hunter, E. P. L.; Lias, S. G. *J. Phys. Chem. Ref. Data* **1998**, *27*, 413.

(15) Murchie, M. P.; Johnson, J. P.; Passmore, J.; Sutherland, G. W.; Tajik, M.; Whidden, T. K.; White, P. S.; Grein, F. *Inorg. Chem*., **1992**, *31*, 273.

(16) Harcourt, R. D. *Qualitative Valence Bond Descriptions of Electron-Rich Molecules: Pauling "3-Electron Bonds" and "Increased-Valence" Theory. Lecture Notes in Chemistry*; Springer: Berlin, 1982; Vol. 30. A July 2003 addendum is available from the author.

(17) (a) Harcourt, R. D. *J. Phys. Chem*. **1991**, *95*, 6916. (b) Harcourt, R. D. *Eur. J. Inorg. Chem*. **2000**, 1901. (c) Harcourt R. D. In *Quantum Chemical Methods in Main-Group Chemistry*; Klapötke T, M., Schulz, A., Eds.; Wiley: New York, 1998; p 232.

(18) See for reviews: (a) Klapötke, T.; Passmore, J. *Acc. Chem. Res*. **1989**, *22*, 234. (b) Burford, N.; Passmore, J.; Sanders, J. C. P. In *From Atoms to Polymers, Isoelectronic Analogies*; Liebman, J. F., Greenberg, A., Eds.; VCH Publishers: Boca Raton, FL, 1989; pp 53−108. (c) Passmore, J. In *Studies in Inorganic Chemistry*; Steudel, R., Ed.; Elsevier: New York, 1992; Vol. 14, pp 373−406. (d) Cameron, T. S.; Deeth, R. J.; Dionne, I.; Du H.; Jenkins, H. D. B.; Krossing, I.; Passmore, J.; Roobottom, H. K. *Inorg. Chem*. **2000**, *39*, 5614. (e) Beck, J. In *Inorganic Chemistry in Focus*; Meyer, G., Naumann, D., Wesemann, L., Eds.; Wiley-VCH: Weinheim, 2005; Vol. 2, pp 35−52.

(19) Leung, Y. C.; Waser, J. *J. Phys. Chem*. **1956**, 60, 539.

structures because in those configurations the positive charge is highly delocalized in contrast to the σ-bonded alternatives, in which the positive charge is formally localized on adjacent atoms.[15] Thus the presence of $np_\pi - np_\pi$ ($n \geq 3$) bonds (and accompanying $\pi^* - \pi^*$ bonds and cagelike geometries) has been accounted for on the basis of positive charge delocalization from the formally positively charged atoms in the classically σ-bonded structure.[10i,18,20]

The structure of $S_2I_4^{2+}$ is also distinctly different from the structure of the heavier chalcogen congener $Se_2I_4^{2+}$, which was first prepared in 1982 as its $Sb_2F_{11}^-$ salt[21] and later as its AsF_6^- salt.[22] The structure of the $Se_2I_4^{2+}$ ion is a distorted triangular prism similar to that of the isolobal approximately C_{2v}-symmetric $S_2O_4^{2-}$ anions in $Na_2[S_2O_4]$ and $Zn[S_2O_4]\cdot$ pyridine.[23] It was proposed that it is formed from two SeI_2^+ radical cations (with a formal Se−I bond order of $1^1/_4$) weakly bonded by a six center two electron, 6c2e, $\pi^* - \pi^*$ bond (see Figure 2)[13] with the Se−I bond distance consistent with a delocalized $3p_\pi - 5p_\pi$ bond (**B** in Figure 3).[22] This description of $Se_2I_4^{2+}$ as a dimer of two SeI_2^+ makes it a subject of further interest. Although salts containing SeI_2^+ have so far not been isolated, the 19 valence electron SeI_2^+ would be a member of a relatively rare class of species, other members of which include O_3^-,[24] NF_2,[25] SO_2^-,[26] or ClO_2,[27] which are all radical AB_2 entities containing 19 valence electrons.

The different structures of $S_2I_4^{2+}$ and $Se_2I_4^{2+}$ have been attributed to the higher S−S π-bond energy compared to that for the Se−Se π bond (see Table 1) and the near equality of the S_2 and I_2 IEs (cf. S_2 (9.40 eV) and I_2 (9.39 eV)) compared to the IE of Se_2 (8.90 eV).[5e,14,22] The bonding in $Se_2I_4^{2+}$ has been investigated previously using HF/STO-3G[22] and VB/STO-5G[17a] calculations using $S_2Cl_4^{2+}$ as a model system and discussed in numerous reviews.[10i,18] In the most recent investigation the bonding in $Se_2I_4^{2+}$ was described as a 10π aromatic system based on calculated nuclear independent chemical shifts.[28]

However, a number of questions remain, i.e., (1) Are the previously proposed bonding models valid for $S_2I_4^{2+}$ and $Se_2I_4^{2+}$? (2) What accounts for the difference in the structures of $S_2I_4^{2+}$ and $Se_2I_4^{2+}$? Are the previous suggestions correct? (3) Why are the classically bonded isolobal P_2I_4 and As_2I_4 structures not adopted? (4) Is the high experimental S−S bond order based on bond distances, stretching frequencies, and force constants supported by theoretical-based bond orders? (5) How does this S−S bond order relate to the high bond orders for the homoatomic bonds between other heavier main group elements, especially that in RSiSiR?

This paper seeks answers to these questions by applying modern electron structure analysis methods including atoms in molecules (AIM) theory,[29,30] natural bond orbital (NBO) theory,[31] valence bond (VB) theory, and direct analysis of molecular orbitals (MOs).

2. Computational Details

All calculations have been carried out with Gaussian 98[32] and Molpro[33] programs. The PBE0 DFT hybrid functional has been used for geometry optimizations,[34] and energy differences have been determined by CCSD(T)[35] single-point calculations on PBE0-optimized structures. In our previous study a large triple-valence basis set was shown to be necessary to reproduce reliable geometries for $S_2I_4^{2+}$.[11] A relativistic effective core potential basis set SDB-cc-pVTZ[36] was used for iodine and tellurium and Dunning's cc-pVTZ basis set[37] for other elements. The methods and basis sets used in optimizations and energy calculations are the same that were used in our previous $S_2I_4^{2+}$ paper.[11] The quality of the calculation methods was established by comparison to experimental ionization energies of diatomic species (see Table 6). Kohn−Sham orbitals from PBE0/6-311G(d) single-point calculations were used

(20) See for reviews: (a) Krossing, I. *Top. Curr. Chem.* **2003**, 230, 135. (b) Sheldrick, W. S. In *Molecular Clusters of the Main Group Elements*; Driess, M., Noeth, H., Eds.; Wiley-VCH: Weinheim, 2004; pp 230−245.

(21) Nandana, W. A. S.; Passmore, J.; White, P. S.; Wong, C.-M. *J. Chem. Soc., Chem. Commun.* **1982**, 1098.

(22) Nandana, W. A. S.; Passmore, J.; White, P. S.; Wong, C.-M. *Inorg. Chem.* **1990**, *29*, 3529.

(23) (a) Kiers, C. T.; Vos, A. *Acta Crystallogr.* **1978**, *B34*, 1499. (b) Dunitz, J. D. *Acta Crystallogr.* **1956**, *9*, 579.

(24) (a) Schnick, W.; Jansen, M. *Angew. Chem.* **1985**, *97*, 48; *Angew. Chem., Int. Ed. Engl.* **1985**, *24*, 54. (b) Schnick, W.; Jansen, M. *Reu. Chim. Miner.* **1987**, *24*, 446. (c) Hesse, W.; Jansen, M.; Schnick, W. *Prog. Solid State Chem.* **1989**, *19*, 47.

(25) Freemann, J. P. Z. *Inorg. Chim. Acta, Reu.* **1967**, *1*, 65.

(26) Clark, H. C.; Horsfield, A.; Symons, M. C. R. *J. Chem. Soc.* **1961**, 7.

(27) (a) Pascal, J.-L.; Pavia, A. C.; Portier, J. *J. Mol. Struct.* **1972**, *13*, 381. (b) Miyazaki, K.; Tanoura, M.; Tanaka, K.; Tanaka, T. *J. Mol. Spectrosc.* **1986**, *116*, 435. (c) Rehr, A.; Jansen, M. *Inorg. Chem.*, **1992**, *31*, 4740. (d) Rehr, A.; Jansen, M. *Angew. Chem.* **1991**, *103*, 1506; *Angew. Chem., Int. Ed. Engl.* **1991**, *30*, 1510.

(28) Zhang, Q.; Lu, X.; Huang, R.; Zheng, L. *Inorg. Chem.* **2006**, *45*, 2457.

(29) Bader, R. W. F. *Atoms in molecules − A quantum theory*; Oxford University Press: Oxford, 1990.

(30) (a) Fradera, X.; Poater, J.; Simon, S.; Duran, M.; Solà, M. *Theor. Chem. Acc.* **2002**, *108*, 214. (b) Fradera, X.; Austen, M. A.; Bader, R. W. F. *J. Phys. Chem. A* **1999**, *103*, 304. (c) Bader, R. W. F.; Stephens, M. E. *J. Am. Chem. Soc.* **1975**, *97*, 7391.

(31) (a) Reed, A. E.; Weinstock, R. B.; Weinhold, F. *J. Chem. Phys.* **1985**, *83*, 735. (b) Reed, A. E.; Curtiss, L. A.; Weinhold, F. *Chem. Rev.* **1988**, *88*, 899. (c) Glendening, E. D.; Badenhoop, J. K.; Reed, A. E.; Carpenter, J. E.; Bohmann, C. M.; Morales, C. M.; Weinhold, F. *NBO*, Version 5.0; Theoretical Chemistry Institute, University of Wisconsin: Madison, WI, 2001.

(32) Frisch, M. J.; Trucks, G. W.; Schlegel, H. B.; Scuseria, G. E.; Robb, M. A.; Cheeseman, J. R.; Zakrzewski, V. G.; Montgomery, J. A., Jr.; Stratmann, R. E.; Burant, J. C.; Dapprich, S.; Millam, J. M.; Daniels, A. D.; Kudin, K. N.; Strain, M. C.; Farkas, O.; Tomasi, J.; Barone, V.; Cossi, M.; Cammi, R.; Mennucci, B.; Pomelli, C.; Adamo, C.; Clifford, S.; Ochterski, J.; Petersson, G. A.; Ayala, P. Y.; Cui, Q.; Morokuma, K.; Malick, D. K.; Rabuck, A. D.; Raghavachari, K.; Foresman, J. B.; Cioslowski, J.; Ortiz, J. V.; Stefanov, B. B.; Liu, G.; Liashenko, A.; Piskorz, P.; Komaromi, I.; Gomperts, R.; Martin, R. L.; Fox, D. J.; Keith, T.; Al-Laham, M. A.; Peng, C. Y.; Nanayakkara, A.; Gonzalez, C.; Challacombe, M.; Gill, P. M. W.; Johnson, B. G.; Chen, W.; Wong, M. W.; Andres, J. L.; Head-Gordon, M.; Replogle, E. S.; Pople, J. A. *Gaussian 98*, Revision A.11; Gaussian, Inc.: Pittsburgh, PA, 1998.

(33) Amos, R. D.; Bernhardsson, A.; Berning, A.; Celani, P.; Cooper, D. L.; Deegan, M. J. O.; Dobbyn, A. J.; Eckert, F.; Hampel, C.; Hetzer, G.; Knowles, P. J.; Korona, T.; Lindh, R.; Lloyd, A. W.; McNicholas, S. J.; Manby, F. R.; Meyer, W.; Mura, M. E.; Nicklass, A.; Palmieri, P.; Pitzer, R.; Rauhut, G.; Schütz, M.; Schumann, U.; Stoll, H.; Stone, A. J.; Tarroni, R.; Thorsteinsson, T.; Werner, H.-J. *MOLPRO*, Revision 2002.6.

(34) (a) Perdew, J. P.; Burke, K.; Ernzerhof, M. *Phys. Rev. Lett.* **1996**, *77*, 3865. (b) Perdew, J. P.; Burke, K.; Ernzerhof, M. *Phys. Rev. Lett.* **1997**, *78*, 1396. (c) Perdew, J. P.; Ernzerhof, M.; Burke, K. *J. Chem. Phys.* **1996**, *105*, 9982. (d) Adamo, C.; Barone, V. *J. Chem. Phys.* **1999**, *110*, 6158.

(35) See for example: (a) Bartlett, R. J. *J. Phys. Chem.* **1989**, *93*, 1697 and references therein. (b) Watts, J. D.; Gauss, J.; Bartlett, R. J. *J. Chem. Phys.* **1993**, *98*, 8718.

(36) (a) Martin, J. M. L.; Sundermann, A. *J. Chem. Phys.* **2001**, *114*, 3408. (b) Bergner, A.; Dolg, M.; Kuechle, W.; Stoll, H. Preuss, H. *Mol. Phys.* **1993**, *80*, 1431.

Table 3. Calculated (PBE0/SDB-cc-pVTZ) Structure Parameters [Å, deg] of Different Conformations of $S_2I_4^{2+}$

	$(S_2I_4)[AsF_6]_2$[a,d]	$(S_2I_4)[SbF_6]_2$[a,d]	**A1**[a]	**A2**[a,b]	**B**	**C**	**D1**[b]	**D2**[c]
S−S′	1.842(4)	1.818(10)	1.857	1.847	2.889	2.734	2.571	2.124
S−I^1	2.827(2)	2.993(4)	2.861	3.077	2.331	2.329	2.344	2.378
S−I^2	3.216(2)		3.349			2.340		
I^1−$I^{2\prime}$	2.603(1)	2.571(2)	2.613	2.608	3.724			
I^1−S−I^2	88.8(1)	90.4(2)	106.5	106.9	110.7	110.7	109.8	107.6
I^1/I^2−S−S′	101.9(2) / 92.5(2)	97.2(2)	103.0 / 90.8	97.1	100.3	101.0 / 102.9	102.8	102.0
I^1−S−S′−$I^{2\prime}$	1.3(1)	0	3.2	0	0	100.4	180.0	180.0
I^1−S−S′−$I^{1\prime}$	−90.5(2)	−93.3(1)	−104.0	−108.1	−113.5	−14.1	65.9	68.9

[a] See ref 11. [b] Saddle point. [c] Partial optimization with S−S′ bond length restricted to that in known 1,2-dication **X**.[43a] [d] X-ray structure.

Table 4. Calculated (PBE0/SDB-cc-pVTZ) Structure Parameters [Å, deg] of Different Conformations of $Se_2I_4^{2+}$

	$(Se_2I_4)[AsF_6]_2$[a,d]	$(Se_2I_4)[Sb_2F_{11}]_2$[a,d]	**A1**	**A2**[b]	**B**	**C**	**D1**[b]	**D2**[c]
Se−Se′	2.840(6)	2.841(2)	2.127	2.109	2.961	2.834	2.724	2.382
Se−I^1	2.455(6)	2.447(8)	2.916	3.195	2.452	2.463	2.467	2.489
Se−I^2			3.583			2.453		
I^1−$I^{2\prime}$	3.637(4)	3.709(4)	2.621	2.612	3.835			
I^1−Se−I^2	104.1(2)	106.2(8)	105.5	105.1	108.0	108.1	107.5	106.5
I^1/I^2−Se−Se′	99.3(8)	100.2(13)	102.4/86.1	94.5	100.3	100.6/101.0	100.9	99.5
I^1−Se−Se′−$I^{2\prime}$	4.2(7)	2.0(3)	4.1	0	0	98.9	180.0	180.0
I^1−Se−Se′−$I^{1\prime}$	−106.0(42)	−108.7(21)	−101.0	−105.5	−110.6	−12.1	69.6	71.4

[a] Averaged values taken from ref 22. [b] Saddle point. [c] Partial optimization with Se−Se′ bond length restricted to that in known 1,2-dication **X**.[43b] [d] X-ray structure

for all bonding analyses. The 6-311G(d) basis set[38] was chosen because it provides an all electron basis set for iodine.

The TopMod code was employed to obtain AIM delocalization indices.[39] Step sizes less than 0.1 au were used in TopMod calculations to produce results accurate to a few percent, which is sufficient for comparison purposes. AIM charges and properties of bond critical points were calculated using AIMPAC.[40] Natural orbital analyses were done using the NBO program (version 5.0).[31c] The highest possible molecular symmetry was used in all calculations, and the results of the bonding analyses were interpreted within the limits of these symmetries. All the theoretical bond orders presented in this paper have been normalized using bonds with reasonably well-defined bond orders. Normalized theoretical bond orders have been used because non-normalized bond orders for bonds of heavier elements are usually significantly lower than those for similar bonds of light elements.[41] This is due to the lower ionization energy and larger size of the heavier elements, which results in more diffuse valence electrons that are not as localized on bonds or electron pairs. The normalization procedure for calculated bond orders is included with the Supporting Information.[42]

3. Results and Discussion

3.1. Calculated Structures. The $S_2I_4^{2+}$ and $Se_2I_4^{2+}$ ions have five calculated stationary points, which correspond to the structures and relative energies of **A1**, **A2**, **B**, **C**, and **D1** presented in Figure 3. Selected structural parameters are given in Tables 3 and 4 (absolute calculated energies are included with the Supporting Information). In addition, the partially optimized trans centrosymmetric **D2** structures, adopted by P_2I_4 and As_2I_4, were calculated as well by constraining the chalcogen−chalcogen bond length to that of an approximate single bond length between two positively charged chalcogen atoms. The experimental single bond lengths found in the 1,5-dichalcogenacyclooctane dications **X** were used for this purpose.[43]

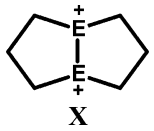

X

The calculated stationary points **A1** and **A2** correspond to the experimental structures of $S_2I_4^{2+}$ found in $(S_2I_4)[MF_6]_2$-(s) (M = As, **A1**; Sb, **A2**)[11,12,15] and reproduce the experimental structure parameters well, apart from the I···S···I angle. It is likely that the larger calculated I···S···I angle reflects the repulsion by the $I^{\delta+}$ iodine atoms and the shallow bending potential energy surface in the gas phase which facilitates the distortion of the angle from the gas-phase value in solid state. This is supported by a partial optimization in C_{2v} symmetry using the I···S···I angle from the experimental structure, which lead only to minor changes in other structure parameters[44] with an energy increase of less than 4.6 kJ/

(37) (a) Dunning, T. H., Jr. *J. Chem. Phys*. **1989**, *90*, 1007. (b) Woon, D. E.; Dunning, T. H., Jr. *J. Chem. Phys*. **1993**, *83*, 1358.
(38) The 6-311G(d) basis set was taken as it is from EMSL basis set library, http://www.emsl.pnl.gov/forms/basisform.html
(39) Noury, S.; Krokidis, X.; Fuster, F.; Silvi, B. *Comput. Chem*. **1999**, *23*, 597.
(40) Bader, R. W. F; et. al. *AIMPAC: A Suite of programs for the AIM theory*; McMaster University: Hamilton, Ontario, Canada L8S 4M1, http://www.chemistry.mcmaster.ca/aimpac/
(41) (a) Llusar, R.; Beltrán, A.; Andrés, J.; Noyry, S.; Silvi, B. *J. Comput. Chem*. **1999**, *20*, 1517. (b) Chesnut, D. B. *Heteroat. Chem*. **2000**, *11*, 341.
(42) A linear dependence was assumed between bond orders and delocalization indices and Mayer bond indices. The relationship between bond orders and ρ_{BCP} values is expected to be of the form: BO = exp [**A** × ρ_{BCP} − **B**].[29] It should be noted that assuming linear dependence far beyond the range of reference bonds is not recommended, as extrapolation leads to unreal bond orders especially for weak bonds.
(43) (a) Iwasaki, F.; Toyoda, N.; Akaishi, R.; Fujihara, H.; Furukawa, N. *Bull. Chem. Soc. Jpn*. **1988**, *61*, 2563. (b) Iwasaki, F.; Morimoto, M.; Yasui, M.; Akaishi, R.; Fujihara, H.; Furukawa, N. *Acta Crystallogr*. **1991**, *C74*, 1463.
(44) Calculated structure parameters from partial optimization of $S_2I_4^{2+}$ cation: S−S, 1.845 Å; S−I, 3.092 Å; I−I, 2.611 Å; I−I−S, 82.9°; S−S−I, 97.1°; I−I−S−S, 0.0°; I−S−S−I, 0.0°.

mol compared to the **A2** structure. C_{2v}-symmetric **A2** structures of both $S_2I_4^{2+}$ and $Se_2I_4^{2+}$ ions are calculated to be saddle points at the PBE0/SDB-cc-pVTZ level with respect to symmetry breaking leading to C_2-symmetric **A1** structures. The **A1**-$Se_2I_4^{2+}$ is somewhat more distorted from C_{2v} symmetry than **A1**-$S_2I_4^{2+}$. For a more detailed discussion of the structures **A1** and **A2** of $S_2I_4^{2+}$, we refer the reader to our previous article.[11]

There is a drastic change in bond lengths and thus bonding going from structures **A** to **B** (Table 3). The multiple E−E and I−I bonds in **A** convert to weak homoatomic interactions (cf. S−S single bond 2.05 Å in S_8,[45] Se−Se single bond 2.325−2.342 Å in Se_8 (298 K)[46]) in **B** structures accompanied with the strengthening of the weak E···I interactions to bonds shorter than conventional single bonds (cf. S−I 2.406(4) Å in $(Ph)_3CSI$[47] and Se−I 2.528(2) Å in 2,4,6-tBu$_3$C$_6$H$_2$SeI[48]). The calculated **B**-$Se_2I_4^{2+}$ structure is in agreement with the structures found in $(Se_2I_4)[AsF_6]_2$(s) and $(Se_2I_4)[Sb_2F_{11}]_2$(s),[22] although the calculated Se−Se distance is about 0.1 Å longer than observed.[49] Structural changes between the **B**, **C**, and **D1** structures, which are governed by rotation of IEI^+ units about the weak E···E bond, are small. Constraining the E−E bond in **D2** structures to single bond length leads to some lengthening of the E−I bonds compared to **D1** structures, but the E−I bonds still remain shorter than typical single bonds. Thus, even though the **D1** and **D2** structures have the same trans conformation as the σ-bonded P_2I_4, their bonding is not classical. The **C** structures resemble those reported for $S_2O_4^{2-}$ in the crystal structure of $Na_2[S_2O_4]\cdot 2H_2O$, and **D1** and **D2** structures have the same centrosymmetric conformation as $S_2O_4^{2-}$ in solution and in solid $(Et_4N)_2[S_2O_4]$, as indicated by spectroscopic measurements.[50]

The calculated **A1** and **A2** structures of both $S_2I_4^{2+}$ and $Se_2I_4^{2+}$ have the same relative energies within the accuracy of the calculations. The global minimum of $S_2I_4^{2+}$ is not unequivocally determined by the present calculations due to the small discrepancy between the relative energies calculated at DFT and CCSD(T) levels.[11] The **B** structure is calculated to be the global minimum for $Se_2I_4^{2+}$, 44.7 kJ/mol lower in energy than the **A** structures, whereas the **B** structure of $S_2I_4^{2+}$ is 16.6 kJ/mol higher in energy than **A1**. The energy differences between **B**, **C,** and **D1** structures are fairly small (energies within 15.1 kJ/mol for $S_2I_4^{2+}$ and within 10.1 kJ/mol for $Se_2I_4^{2+}$), indicating only small changes in bonding going from one isomer to another. The very approximately σ-bonded **D2** structure is the highest energy structure for $S_2I_4^{2+}$, while the **A** structures remain the highest energy structures for $Se_2I_4^{2+}$.

The relatively small energy differences between some of the structures raises the question whether the calculated energy order is correct or could it be different from the experimental order in the solid state. In principle the situation in the solid-state could be modeled with the calculations by adding counterions and using periodic boundary conditions to model the crystal structure.[51] Unfortunately, due to the heavy atoms and the number of atoms involved, such calculations are beyond the scope of our resources. However, for the following reasons, it seems unlikely that the energy ordering of the different structures would change from the calculated order. (1) The calculated relative energies do not change significantly upon changing the calculation method or basis set (see Supporting Information). (2) In the experimental structures of $(S_2I_4)[MF_6]_2$ (M = As, Sb),[11] $(Se_2I_4)[Sb_2F_{11}]$,[21] and $(Se_2I_4)[AsF_6]_2$[22] all interionic interactions are weak and numerous, ideal for the retention of the gas-phase properties of the dications in the solid state, and accordingly, the calculated global minimum structures of both cations are well matched by respective experimental structures in the solid state. (3) The optimized structures and their relative energies are in line with the proposed simple bonding models giving a coherent and consistent picture of the bonding in $S_2I_4^{2+}$ and $Se_2I_4^{2+}$, as will be shown in the following sections.

3.2. The Nature of the Bonding in $S_2I_4^{2+}$ and $Se_2I_4^{2+}$. 3.2.1. AIM Analysis. Full AIM analyses were carried out for **A**, **B**, **D1**, and **D2** conformations of $S_2I_4^{2+}$ and $Se_2I_4^{2+}$ and of I_4^{2+} and $(S_2^+)_2$ for comparison. The electron densities are given in Figure 4, and the properties of AIM critical points,[52] AIM charges, and bond orders in Figures 5 and 7−10. In addition, the properties of E−I bond critical points (BCPs) in model species EI_2^+, EI_3^+, and Me_3CEI (E = S, Se) were determined as references of sulfur iodine and selenium iodine bonds and are presented in Figures 8 and 9 and Table 5. The AIM analysis showed seven BCPs and two ring critical points for the **A** and **B** conformations and five BCPs for the **D1** and **D2** conformations in accordance with the Poincaré−Hopf relationship.[53]

3.2.1.1. A-$S_2I_4^{2+}$. The AIM bond critical point density (ρ_{BCP})-based bond orders and charges (see Figure 5) are in good agreement with those predicted by the simple bonding

(45) Rettig, S. J.; Trotter, J. *Acta Crystallogr*. **1987**, *C43*, 2260.
(46) Cherin, P.; Unger, P. *Acta Crystallogr*. **1972**, *B28*, 313. (b) Burbank, R. D. *Acta Crystallogr*. **1952**, *5*, 236. (c) Foss, O.; Janickis, V. *J. Chem. Soc., Dalton Trans*. **1980**, 624. (d) Maaninen, A.; Konu, J.; Laitinen, R. S.; Chivers, T.; Schatte, G.; Pietikainen, J.; Ahlgren, M. *Inorg. Chem*. **2001**, *40*, 3539. (e) Maaninen, T.; Konu, J.; Laitinen, R. S. *Acta Crystallogr*. **2004**, *E60*, o2235.
(47) Minkwitz, R.; Preut, H.; Sawatzki, J. Z. *Naturforsch*. **1988**, *43b*, 399.
(48) Du Mont, W. W.; Kubiniok, S.; Peters, K.; Von Schnering, H. G. *Angew. Chem*. **1987**, *99*, 820; *Angew. Chem., Int. Ed. Engl*. **1987**, *26*, 780.
(49) (a) The longer calculated Se−Se distance is attributed to the common tendency of DFT calculations to overestimate weak bonds. This is due to the inability of present DFT functionals to treat the dispersion forces that are important for the description of weak bonds. A similar trend is observed for the calculated S−I bond lengths in **A**-$S_2I_4^{2+}$. (b) Koch, W.; Holthausen, M. C. *A Chemist's Guide to Density Functional Theory*, 2nd ed.; Wiley-VHC: Weinheim, 2001.
(50) (a) Weinrach, J. B.; Meyer, D. R.; Guy, J. T., Jr.; Michaelski, P. E.; Carter, K. L.; Grubisha, D. S.; Bennett, D. W. *J. Crystallogr. Spectrosc. Res*. **1992**, *22*, 291. (b) Hodgeman, W. C.; Weinrach, J. B.; Bennett, D. W. *Inorg. Chem*. **1991**, *30*, 1611.
(51) Young, D. C. *Computational Chemistry*; Wiley-Interscience: New York, 2001.
(52) The critical points of the electron density are classified in AIM theory as bond critical points (BCPs), nuclear critical points (NCPs), ring critical points (RCPs), and cage critical points (CCPs). BCPs are most important for AIM theory, as their properties are used to define the properties of bonds.[29]
(53) The Poincaré −Hopf relationship states that number of NCP − number of BCP + number of RCP − number of CCP = 1.[29]

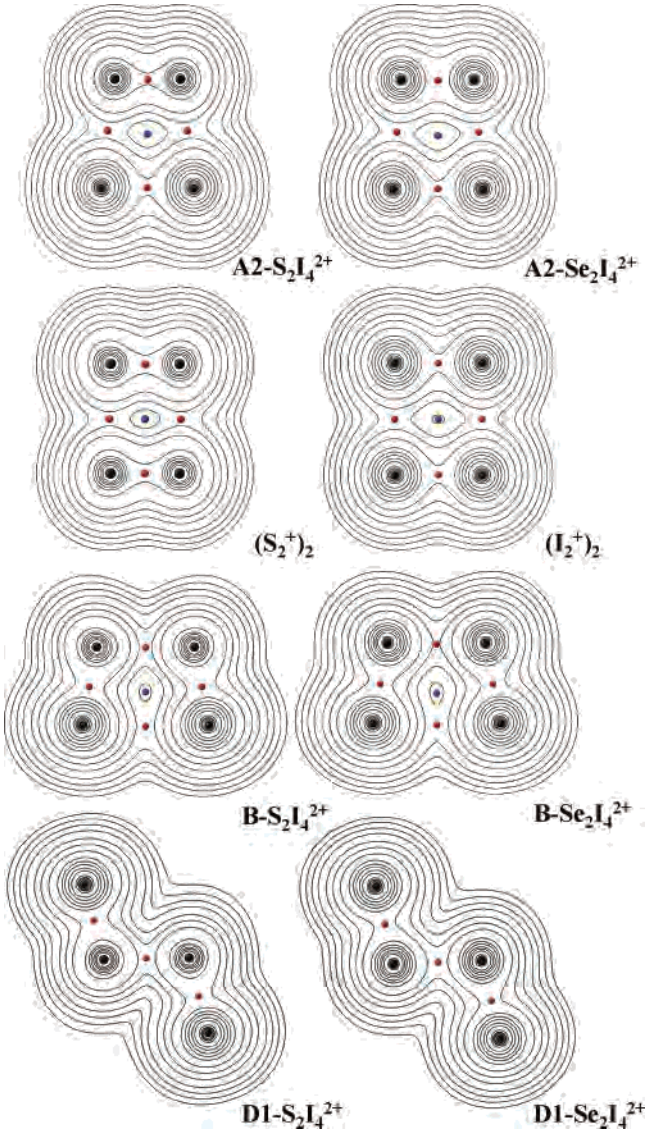

Figure 4. Comparison of calculated electron densities and AIM critical points ($I^1EE'I^{2'}$ plane) of **A2**, **B**, and **D1** conformations with those of $(S_2^+)_2$ and I_4^{2+}. The outermost contour value is 0.001, and the other contours are 2×10^n, 4×10^n, and 8×10^n ($n = -3, -2, ..., 2$). Color legend: nuclear critical points (black), bond critical points (red), and ring critical points (blue).

model (see Figure 1). The calculated electron densities (see Figure 4) and properties of BCPs of **A**-$S_2I_4^{2+}$, $(S_2^+)_2$, and I_4^{2+} (see Table 5) are very similar, establishing that they also have similar bonding.

The simpler $(S_2^+)_2$ and I_4^{2+} can be described by two X_2^+ (X = S, I) units weakly bound together by $\pi^*-\pi^*$ bonds;[55] thus, the bonding in **A**-$S_2I_4^{2+}$ can be viewed as arising from two I_2^+ interacting with S_2 via two mutually perpendicular $\pi^*-\pi^*$ orbitals, followed by positive charge delocalization (see Figure 1). All atoms have approximately equal positive charges and are of almost equal electronegativity, and thus,

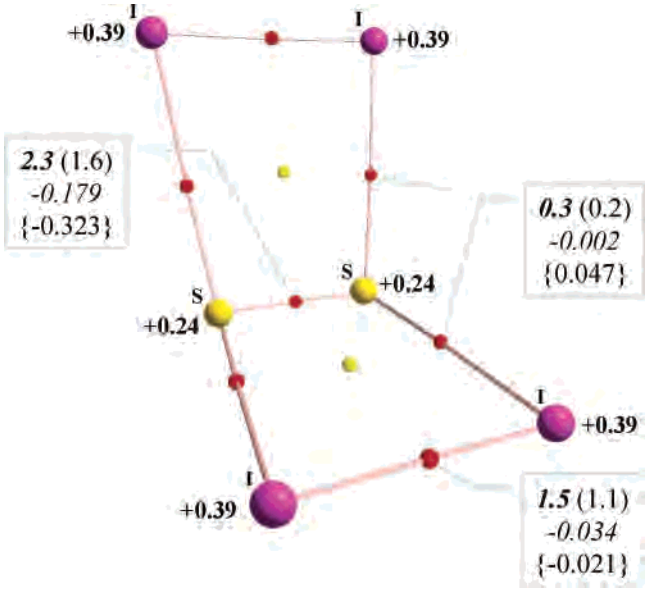

Figure 5. AIM charges (bold) and properties of AIM bond critical points of **A**-$S_2I_4^{2+}$: bond orders based on critical point density, ρ_{BCP} (bold italic), and delocalization index, δ (in brackets), kinetic energy density, H_{BCP} (italic), and Laplacian $\nabla^2\rho_{BCP}(\mathbf{r})$ {in brackets}. Color legend: bond critical points (red), ring critical points (small yellow), sulfur (large yellow), selenium (gold), and iodine (purple).

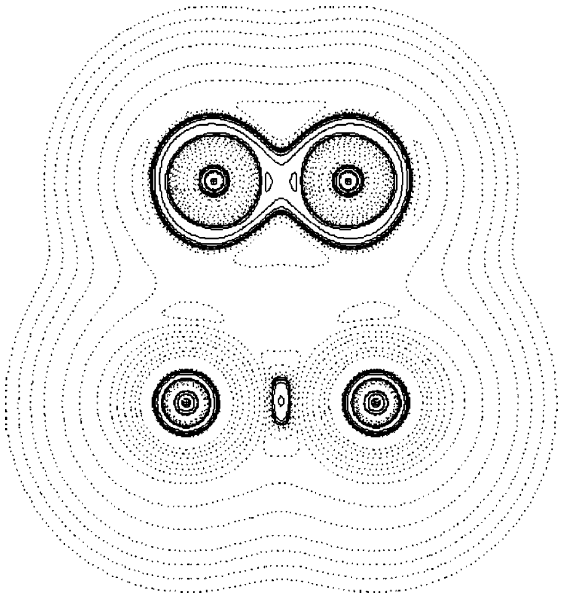

Figure 6. Laplacian of the electron density ($I^1EE'I^{2'}$ plane) of **A**-$S_2I_4^{2+}$. Contour values are drawn at ± 0.001, $\pm 2 \times 10^n$, $\pm 4 \times 10^n$, and $\pm 8 \times 10^n$ ($n = -3, -2, ..., 2$). Negative contour values are marked with dotted line.

covalent bonding between atoms is expected. In AIM theory covalent bonding interactions are normally indicated by negative Laplacian $\nabla^2\rho_{BCP}(\mathbf{r})$ values.[29] This is the case for S−S and I−I but not for the weak S−I bonds. It has been shown by Macchi and Sironi in their recent review that small positive Laplacian values are not uncommon for covalent bonds between heavy elements.[56] A contour plot of the Laplacian of **A**-$S_2I_4^{2+}$ in Figure 6 illustrates the characteristics associated with compounds of heavy atoms[56] and the relative featurelessness of electron density between sulfur and iodine atoms which results in the small positive $\nabla^2\rho_{BCP}(\mathbf{r})$ value

(54) Krossing, I.; Passmore, J. *Inorg. Chem.* **1999**, *38*, 5203.
(55) The structure of rectangular I_4^{2+} has been shown to result from the formation of a weak 4c2e $\pi^*-\pi^*$ bond between the singly occupied antibonding π^* MOs of two I_2^+ monomers.[10i,15,18b] The bonding of the rectangular high-energy isomer of S_4^{2+} $(S_2^+)_2$ was described by a similar 4c2e $\pi^*-\pi^*$ bond.[54] For MO and VB descriptions of I_4^{2+}, see also Harcourt, R. D. *J. Mol. Struct. THEOCHEM* **1985**, *122*, 235.
(56) Macchi, P.; Sironi, A. *Coord. Chem. Rev.* **2003**, *238−239*, 383.

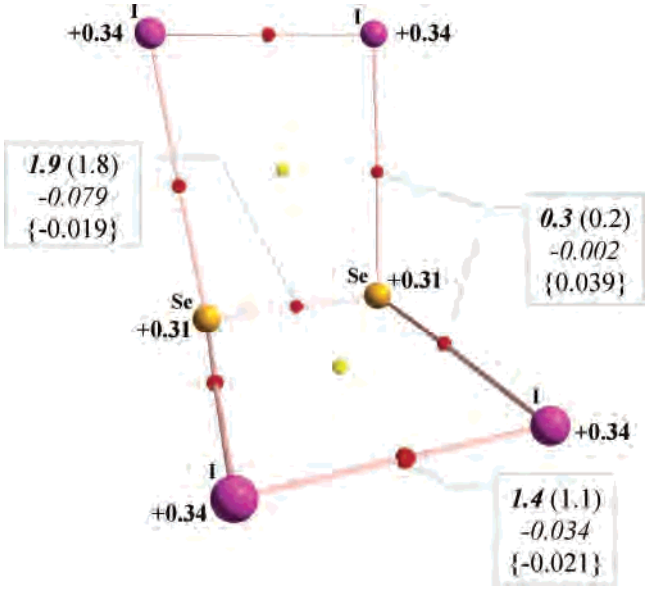

Figure 7. AIM charges and properties of AIM bond critical points of **A**-$Se_2I_4^{2+}$. For the color code and an explanation of different numbers, see the caption of Figure 5.

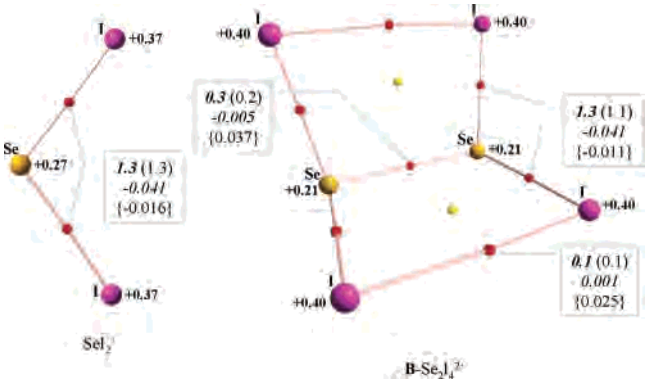

Figure 8. AIM charges and properties of AIM bond critical points of SeI_2^+ and **B**-$Se_2I_4^{2+}$. For the color code and an explanation of different numbers, see the caption of Figure 5.

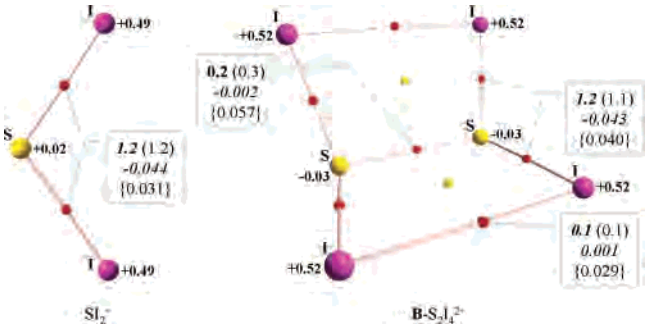

Figure 9. AIM charges and properties of AIM bond critical points of SI_2^+ and **B**-$S_2I_4^{2+}$. For the color code and an explanation of different numbers, see the caption of Figure 5.

for the S−I bonds. Cremer and Kraka have introduced the electronic energy density $H(\mathbf{r})$ as a measure of covalency in bonds to remedy the difficulty associated with interpreting the positive values of $\nabla^2\rho_{BCP}(\mathbf{r})$ found for bonds where shared interactions are expected.[57] Electronic energy density $H(\mathbf{r})$ has been shown to be negative for shared interactions even between heavy atoms.[56,58] Consequently, all H_{BCP} values are negative for **A**-$S_2I_4^{2+}$, confirming the expected covalent

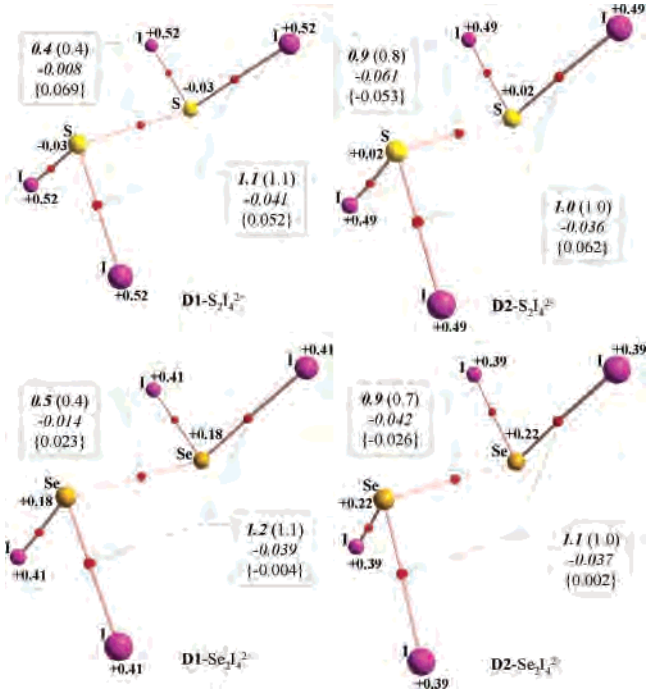

Figure 10. AIM charges and properties of AIM bond critical points of **D1**-$S_2I_4^{2+}$, **D2**-$S_2I_4^{2+}$, **D1**-$Se_2I_4^{2+}$, and **D2**-$Se_2I_4^{2+}$. For the color code and an explanation of different numbers, see the caption of Figure 5.

Table 5. AIM Bond Parameters of Selected Sulfur, Selenium, and Iodine Species

	bond	ρ_{BCP}	δ(A,B)	H_{BCP}	$\nabla^2\rho_{BCP}$
$(S_2^+)_2$	$(S-S)_{short}$	2.5	2.2	−0.202	−0.380
	$(S-S)_{long}$	0.2	0.3	−0.002	0.054
I_4^{2+}	$(I-I)_{short}$	1.5	1.2	−0.034	−0.016
	$(I-I)_{long}$	0.2	0.2	−0.001	0.036
SI_3^+	S−I	1.0	0.9	−0.035	0.042
Me_3CSI	S−I	1.0	1.0	−0.036	0.000
SeI_3^+	Se−I	1.0	1.0	−0.032	−0.046
Me_3CSeI	Se−I	1.0	1.0	−0.029	−0.009

nature of the bonds. The overall AIM analysis for **A**-$Se_2I_4^{2+}$ (see Figure 7) is similar to that of **A**-$S_2I_4^{2+}$.

The S−S ρ_{BCP} bond order is in good agreement with the simple bond model, while the I−I ρ_{BCP} bond order is slightly higher than that predicted by the simple bond model for the I−I bond order. On the other hand, the delocalization index δ(A,B)-based bond orders fail to produce the expected bond orders. Reasons for this failure will be discussed in Section 3.4. The AIM analysis also gives bond order estimates for the weak S−I bonds, which cannot be obtained by the simple bond model. The S−I bond orders predicted by both ρ_{BCP} and δ(A,B) are in good agreement with the weak 4c2e bonds in I_4^{2+} and $(S_2^+)_2$ (Table 5). The largest deviation from the simple bonding model comes from calculated atomic charges, which predict the positive charge to lie more on iodine atoms, while the simple bonding model predicted equal charge distribution.

3.2.1.2. B-$Se_2I_4^{2+}$. A comparison of AIM bond parameters and atomic charges in **B**-$Se_2I_4^{2+}$ and SeI_2^+ are presented

(57) (a) Cremer, D.; Kraka, E. *Angew. Chem.* **1984**, *96*, 612; *Angew. Chem., Int. Ed. Engl.* **1984**, *23*, 627; (b) Cremer, D.; Kraka, E. *Croat. Chem. Acta* **1984**, *57*, 1259.
(58) Cortés-Guzmán, F.; Bader, R. F. W. *Coord. Chem. Rev.* **2005**, 249, 633. Erratum Bader, R. F. W. *Coord. Chem. Rev.* **2005**, *249*, 3198.

in Figure 8. The ρ_{BCP}-based bond orders depict similar bond orders for Se−I bonds in **B**-$Se_2I_4^{2+}$ and SeI_2^+. On the other hand, the delocalization index δ-based bond orders reveal a small but distinct decrease in bond order and the atomic charges show some charge transfer from selenium to iodines upon dimerization. These results imply that the SeI_2^+ units in **B**-$Se_2I_4^{2+}$ do not stay as invariable as the simple bonding model might suggest (see Figure 2).

The individual AIM bond orders for bonds between the SeI_2^+ moieties are very small in accordance with the long bond lengths. However, the sum of the bond orders of I···I and Se···Se contacts (0.4−0.5) is similar to the sums of the bond orders of weak S···S (0.4−0.6) and I···I (0.4) contacts in $(S_2^+)_2$ and I_4^{2+}, respectively. This indicates that the bonding between SeI_2^+ units is of similar strength to that between S_2^+ and I_2^+ units in $(S_2^+)_2$ and I_4^{2+}, respectively, which is in agreement with the formation of a 6c2e $\pi^*-\pi^*$ bond as suggested by the simple bonding model (see Figure 2). Note that even though the I···I bond orders in **B**-$Se_2I_4^{2+}$ are nonzero the small positive H_{BCP} values suggest that they are borderline cases to be considered as covalent bonding interaction. Their small but stabilizing contribution to the structure is manifested by the relatively small energy differences between **B** and **D1** conformations. The bonding analysis of **B**-$S_2I_4^{2+}$ (see Figure 9) produces similar results to that of **B**-$Se_2I_4^{2+}$.

3.2.1.3. D Structures. The AIM results for the **D1** and **D2** structures of $S_2I_4^{2+}$ and $Se_2I_4^{2+}$ are presented in Figure 10. The AIM bond orders for the approximately singly bonded **D2** structures are similar or slightly higher than those for the E−I reference bonds and slightly smaller than those for the E−E reference bonds. The calculated AIM charges in the **D2** structures indicate that the positive charge is not located on the tricoordinate chalcogen atoms as expected on the basis of a simple Lewis structure.[59] In **D2**-$S_2I_4^{2+}$ the positive charge is similarly distributed as in SI_2^+ (see Figure 9), and in **D2**-$Se_2I_4^{2+}$ the positive charge on the iodine atoms is even increased with respect to SeI_2^+ (see Figure 8). This shows that even in the **D2** structures, which are forced to be approximately singly bonded, the bonding is nonclassical and different to that predicted by the simple Lewis bonding model and found in the experimental structures of isoelectronic P_2I_4 and As_2I_4. The AIM bond orders in the **D1** structures are between those for the **D2** and **B** structures (see Figures 8−10). The AIM atomic charges are similar in **B**, **D1**, and **D2** structures, while the positive charge is more delocalized in **A** structures. The positive charge also is more delocalized in all structures of $Se_2I_4^{2+}$ than in the structures of $S_2I_4^{2+}$. This infers that the delocalization of positive charge acts as a driving force toward the **A** structures from the other structures and is probably a bigger factor contributing to the stability of the **A**-$S_2I_4^{2+}$ compared to the other structures than is the case for **A**-$Se_2I_4^{2+}$ because the positive charge is already delocalized to some extent in the other $Se_2I_4^{2+}$ structures.

3.2.2. Molecular Orbital Description of the Bonding. A qualitative FMO description of bonding was the basis for deriving the simple $\pi^*-\pi^*$ bonding model for $S_2I_4^{2+}$ and $Se_2I_4^{2+}$ (see Figures 1 and 2). Herein we show that this simple model for both **A**-$S_2I_4^{2+}$ and **B**-$Se_2I_4^{2+}$ is supported by a full quantitative MO analysis.

3.2.2.1. A-$S_2I_4^{2+}$. The 15 lower-energy MOs of the total 18 p-valence MOs of **A**-$S_2I_4^{2+}$ derived from mixing of the MOs of S_2 [6 MOs] and two I_2^+ [2 × 6 MOs] are illustrated in Figure 11. In agreement with the simple MO model for $S_2I_4^{2+}$ (see Figure 1), the effective bonding between S_2 and two I_2^+ (labeled in green and blue in Figure 11) arise from mixing of the two perpendicular SOMOs of S_2 and the two highest energy π^* I_2^+ MOs. These combine to give the bonding MOs 117 and 119, the corresponding antibonding MOs 122 and 123, and the nonbonding MOs 120 and 121. The MOs 120 (98% π^*(I−I)) and 121 (90% π^*(I−I)) are almost pure diiodine π^* antibonding orbitals and thus nonbonding with respect to the S−I contacts. The overall bonding in MOs 117 and 119 can be described either as 6c4e bonding over the whole ion, or by two 4c2e bonds between S_2 and each I_2^+ fragment as in the simple model. These 4c2e $\pi^*-\pi^*$ bonds between S_2 and I_2^+ fragments are by nature substantially weaker than normal covalent single bonds, as manifested by the long S−I distances and AIM parameters for these contacts.

MO theory provides an approximate estimate of bond orders by assuming that a division between bonding, antibonding, and nonbonding orbitals can be made in an unambiguous manner. Summation of the bonding and antibonding π-electron contributions to each of the MOs of **A**-$S_2I_4^{2+}$ shows that it has $3^1/_2$ electrons in bonding S−S π orbitals and 1 electron in antibonding S−S π^* orbitals, resulting in $2^1/_2$ effective bonding π-electrons giving $1^1/_4$ effective S−S π bonds. There are also $3^3/_4$ electrons in bonding I−I π orbitals and $3^1/_4$ in antibonding I−I π^* orbitals, which lead to an effective π-bond order of $^1/_4$ for each I−I bond. The total bond orders of $2^1/_4$ and $1^1/_4$ for S−S and I−I bonds are in good agreement with the experimental-based bond orders given in our previous study[11] and by the simple bonding model (see Figure 1). We have not estimated the bond orders of the weak S···I contacts because of the difficulty of dividing the MOs into σ and π contributions with respect to these bonds. In conclusion, the full MO analysis fully confirms the previously proposed simple frontier molecular orbital results.[15]

3.2.2.2. B-$Se_2I_4^{2+}$. The structure of **B**-$Se_2I_4^{2+}$ can be described as a weakly bonded dimer of two SeI_2^+ ions. In the simple MO picture, the SeI_2^+ ion is formed from σ-bonded SeI_2 by removal of one electron from the π^*-antibonding HOMO[60] accompanied by a rise of the Se−I bond order from 1 to $1^1/_4$. As illustrated in Figure 12, the removal of the electron is followed by relaxation of the π^*-antibonding SOMO and the corresponding π-bonding MO 66 in order

(59) However, note that the calculated charges (including AIM) are lower than expected, e.g., the AIM charge on sulfur in SI_3^+ is −0.10 (the expected simple Lewis charge for tricoordinate sulfur is +1) and on selenium in SeI_3^+ is +0.21.

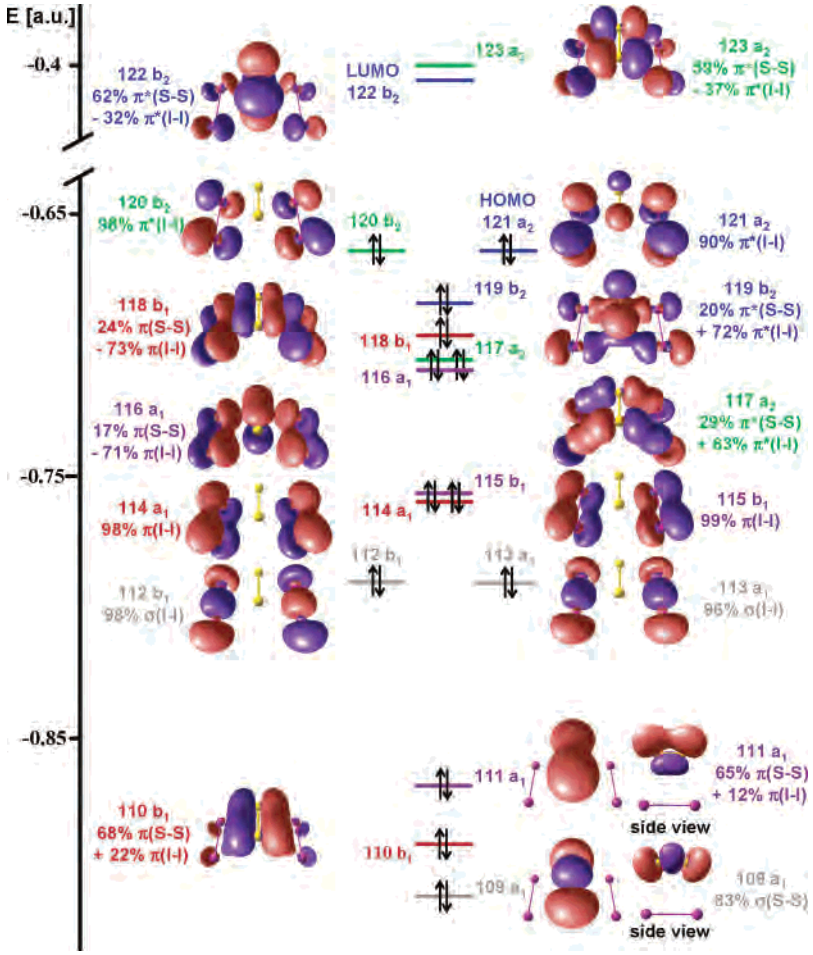

Figure 11. Valence orbitals of **A**-$S_2I_4^{2+}$ (isosurfaces 0.05). Different colors denote the bonding−nonbonding−antibonding combinations between different orbitals of S_2 and I_2^+ units. (+ and − signs indicate whether the interaction between S_2 and I_2^+ fragment orbitals is bonding or antibonding, respectively). The higher-energy MOs 124, 125, and 126 are the antibonding equivalents of the S−S σ bond MO 109 and I−I σ bond MOs 112 and 113 and are included with the Supporting Information.

to minimize the electrostatic repulsion, resulting in positive charge delocalization from selenium onto the iodines.

In the simple bonding model, the bonding of **B**-$Se_2I_4^{2+}$ is characterized by the HOMO (see Figure 13), which is formed by mixing of the π^* SOMOs of the SeI_2^+ moieties resulting in the occupied $\pi^*-\pi^*$ bonding combination (the LUMO is the corresponding antibonding combination). According to the model the contributions from other SeI_2^+ π orbitals to the intradimer bonding should be neglible as both the bonding and antibonding combination are filled. In a recent article,[28] this view was challenged and suggested that the full set of π orbitals should be used to describe the bonding between SeI_2^+ units as a 6c10e bond rather than the 6c2e bond as described by the simple bonding picture. The set of valence MOs in Figure 13 shows that the combinations of lower SeI_2^+ π orbitals (MO 127, MO 132, MO 133, and MO 138) do not fully cancel and do have a contribution to the intradimer bonding. Therefore, for an accurate description of the bonding of **B**-$Se_2I_4^{2+}$, the inclusion of the lower orbitals is warranted. However, it should be noted that the description of the 6c10e bond is not the full picture of bonding either because of the σ/π mixing exhibited by the **B**-$Se_2I_4^{2+}$ MOs, which results in small Se−Se and I−I σ-(anti)bonding contributions from other orbitals (e.g., MO 130 and MO 136).

The quantitative description of bonding requires the inclusion of all valence orbitals. However, at a qualitative level the 6c4e and 6c2e bonding models inferred by the shape of the HOMOs in **A**-$S_2I_4^{2+}$ and **B**-$Se_2I_4^{2+}$ are valid, as they explain the weakness and delocalized nature of the bonds between S_2 and I_2^+ units and between SeI_2^+ units, respectively. Although the inclusion of all valence orbitals leads to a more accurate description of the bonding, it also means losing the predictive power and clarity of the simple bonding model. Therefore, the simple $\pi^*-\pi^*$ bonding model at the qualitative level is a valid and useful approach to describe the bonding in $S_2I_4^{2+}$ and $Se_2I_4^{2+}$, as well as in other related species of electron-rich elements, e.g., $S_6N_4^{2+}$,[61] Te_6^{4+},[10i,18b,c,20b] M_8^{2+} (M = S, Se),[18b−d,20] and $O_2Cl_2^+$.[62]

The Se−I bond orders cannot be determined from the MO analysis for **B**-$Se_2I_4^{2+}$ due to the σ/π mixing of the orbitals. The closest approximation for the Se−I bond orders come from the simple bond model giving the same Se−I bond order $1^1/_4$ as in the SeI_2^+ monomer. This further emphasizes the strength of the simple model because, even though the full MO description reveals differences to the simple model, the differences cannot be quantified.

(60) It should be noted that the classification of the SeI_2 HOMO and the SeI_2^+ SOMO as π^* orbitals stretches the definition of π orbitals. In a strict sense, the definition of π orbitals is limited to linear molecules. However, the π^* orbital notation is used here because these MOs are π symmetric antibonding orbitals with respect to both Se−I bonds.

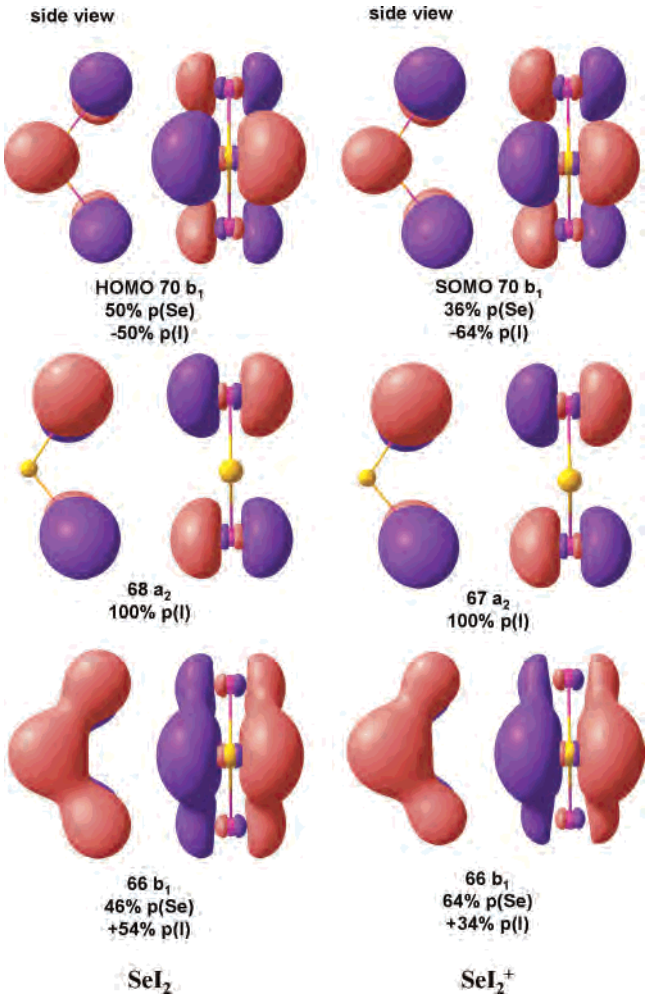

Figure 12. Occupied π orbitals of SeI_2 and SeI_2^+ (isosurfaces 0.05). (+ and − signs indicate whether the interaction between atomic orbitals is bonding or antibonding, respectively).

3.2.3. Valence Bond Description of the Bonding. The qualitative VB model provides a complementary approach to molecular orbital theory in describing the electronic structure of $S_2I_4^{2+}$.[16] In this section the resonance between the increased-valence structures **1**−**4** (Scheme 1)[16,17] is shown to be sufficient to describe the electronic structure of $S_2I_4^{2+}$.

The ground-state MO configurations for the valence-shell π-electrons of S_2 and I_2^+ are given by eqs 1, 3, and 5

$$S{-}S(\pi) = (\pi_{xAB})^2(\pi^*_{xAB})^1(\pi_{yAB})^2(\pi^*_{yAB})^1 \quad (1)$$

$$\propto (p_{xA})^1(\pi_{xAB})^1(p_{xB})^1(p_{yA})^1(\pi_{yAB})^1(p_{yB})^1 \quad (2)$$

$$I_C - I_D(\pi) = (\pi_{xCD})^2(\pi^*_{xCD})^1(\pi_{yCD})^2(\pi^*_{yCD})^2 \quad (3)$$

$$\propto (p_{xC})^1(\pi_{xCD})^1(p_{xD})^1(p_{yC})^2(p_{yD})^2 \quad (4)$$

$$I_E - I_F(\pi) = (\pi_{xEF})^2(\pi^*_{xEF})^2(\pi_{yEF})^2(\pi^*_{yEF})^1 \quad (5)$$

$$\propto (p_{xE})^2(p_{xF})^2(p_{yE})^1(\pi_{yEF})^1(p_{yF})^1 \quad (6)$$

in which π_x and π^*_x and π_y and π^*_y are pairs of bonding and antibonding π-electron MOs—for example $\pi_{xAB} = p_{xA} + p_{xB}$ and $\pi^*_{xAB} = p_{xA} - p_{xB}$. With one S−S or I−I electron-pair σ bond, the S−S and I−I bond orders [BO (SS) and BO (II)] for these configurations are equal to 2.0 and 1.5, respectively. Using the procedure described in ref 63, the $S = 1$ or $S = 1/2$ spin wavefunctions for eqs 1, 3, and 5 can be transformed to give eqs 2, 4, and 6, respectively, from which the π-electron distributions of VB structures **5**, **6**, and **7** are obtained.[16,17] It is assumed that the parallel ($m_s = +1/2$) spins for the π^*_x and π^*_y electrons of S_2 are opposed to that for the singly occupied MO of each I_2^+. When the unpaired antibonding π^*_x and π^*_y electrons of ground-state S_2 are spin-paired with the unpaired electron (π^*_x or π^*_y) of the ground-state for each I_2^+ cation, VB structure **1** for $S_2I_4^{2+}$, as $I_2^+ + S_2 + I_2^+$, is obtained.[16,17] It contains two cyclic 6e4c bonding units—one for the $S_A{-}S_B{-}I_C{-}I_D$ π_x and π^*_x electrons and one for the $S_A{-}S_B{-}I_E{-}I_F$ π_y and π^*_y electrons. Each cyclic 6e4c bonding unit is equivalent to resonance between four canonical Lewis structures. For example, the $S_A{-}S_B{-}I_C{-}I_D$ of **1**, as in **8**, is equivalent to resonance between the Lewis structures **9**−**12** (Scheme 2). Structures **9** and **12** have one nearest-neighbor S−I bond. This type of bond is absent in structures **10** and **11**. Therefore, the nearest-neighbor S−I bond orders in increased-valence structure **1** are substantially less than unity to account for the occurrence of long S−I bonds in $S_2I_4^{2+}$.

The cyclic 6e4c-bonding VB structure **8** participates in resonance with the cyclic 6e4c VB structure **13** (Scheme 2). The latter structure is equivalent to resonance between the Lewis structures **10**, **11**, **14**, and **15**. The $S_2I_4^{2+}$ VB structures **2** and **3** involve one of each of the 6e4c VB structures **8** and **13**. The S−S bond order for VB structure **1** is 2, and the maximum value for the S−S bond order for each of the increased-valence structures **2** and **3** is 2.5. Therefore, resonance between only increased-valence structures **1**, **2**, and **3** cannot account for a higher bond order than 2.5 for the S−S bond in $S_2I_4^{2+}$. To improve further the model, resonance with the increased-valence structure **4** involving two cyclic 6e4c-bonding units of type **13** is included.

Alternatively, the increased-valence structures **1**−**4** can be derived from familiar Lewis octet VB structures, e.g., **1** can also be constructed from the Lewis octet structure **I** of Scheme 3 by one-electron delocalization of nonbonding iodine and sulfur electrons into bonding I−I and S−S MOs, as indicated. The Lewis octet structures **II** ($S_2I_2^{2+} + I_2$), **III** ($I_2 + S_2I_2^{2+}$), and **IV** ($I_2 + S_2^{2+} + I_2$) can be similarly used to construct increased-valence structures **2**, **3**, and **4** via one-electron delocalization.

The final VB representation of the electronic structure of $S_2I_4^{2+}$ is provided by resonance between increased-valence structures **1**, **2**, **3**, and **4** (Scheme 1).[64] The relative weights of the four structures **1**−**4** can be determined on the basis of the bond-order estimates of S−S and I−I bonds, as well as of the S−I bond order. However, the weights strongly depend on the assumed bond orders, e.g., BO (SS) = 2.33, BO (II) = 1.33, and BO (SI) = 0.15 results in the weights for the four resonance structures $W_1 = 0.0089$, $W_2 = W_3 =$

(61) Rawson, J. M.; Palacio, F. *Struct. Bonding* **2001**, *100*, 93.
(62) Drews, T.; Koch, W.; Seppelt, K. *J. Am. Chem. Soc.* **1999**, *121*, 4379.
(63) Green M.; Linnett, J. W. *J. Chem. Soc.* **1960**, 4959.
(64) It can be demonstrated that the wavefunctions for VB structures **8** and **13** are not orthogonal (cf. ref 16, p 146 for example). Therefore, the wavefunctions for VB structures **1**−**4** are not orthogonal. An increased-valence structure for a 6e4c bonding unit possesses a 4c2e bond and two 2c1e bonds.

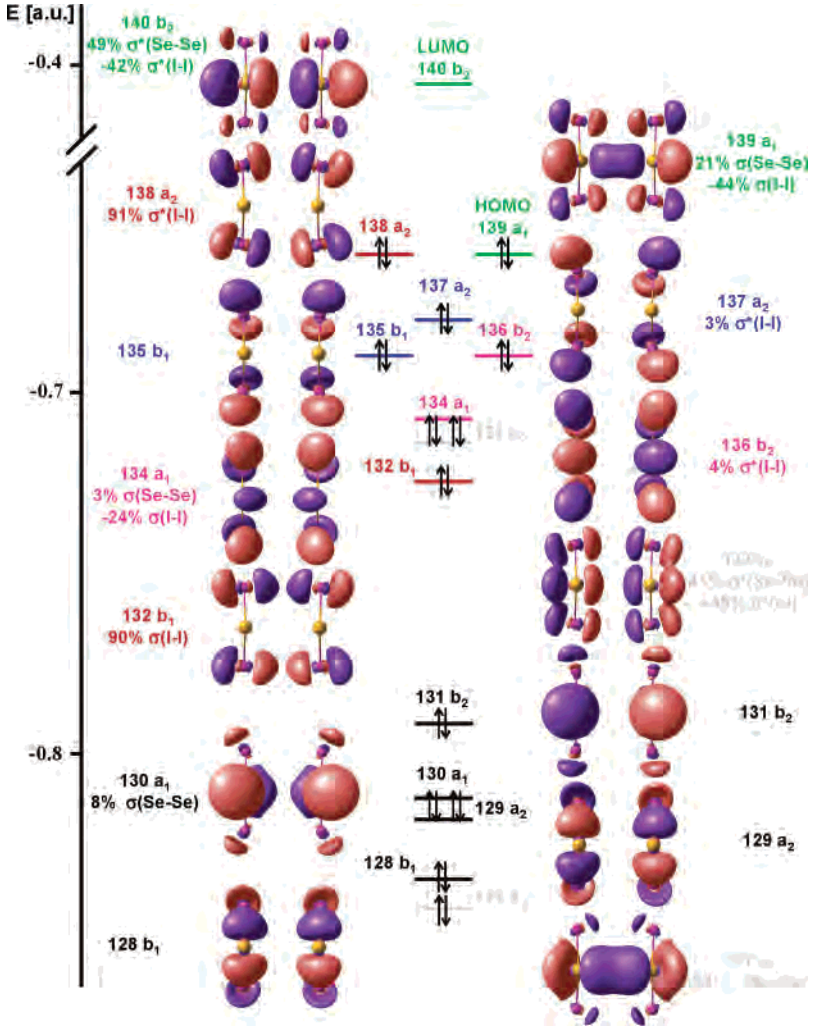

Figure 13. Valence molecular orbitals of **B**-$Se_2I_4^{2+}$ (isosurfaces 0.05). The bonding−antibonding combinations of different SeI_2^+ orbitals are shown with respective colors. Combinations of predominantly SeI_2^+ σ orbitals are marked with black (+ and − signs indicate whether the interaction between Se_2 and I_2^+ fragment orbitals is bonding or antibonding, respectively).

Scheme 1. Thick and Thin Bond Lines Represent Normal and Fractional Electron-Pair Bonds, Respectively, and Dots Represent One-Electron Bonds. Crosses and Circles Are Used to Represent Electrons with $m_s = +1/2$ and $m_s = -1/2$ Spin Quantum Numbers[16,17,63]

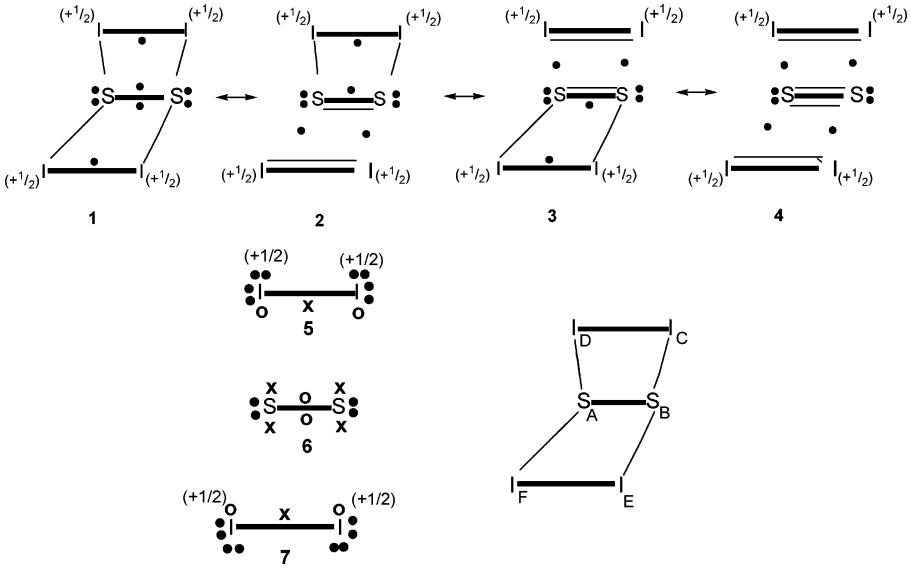

0.4431, and $W_4 = 0.1050$, while BO (SI) = 0.194 leads to significantly different weights $W_1 = 0.3189$, $W_2 = W_3 = 0.3404$, and $W_4 = 0.0003$. Both possibilities are essentially VB equivalents of the simple FMO model shown in Figure 1. A detailed approach describing how to estimate the relative weights is provided in the Supporting Information.

Scheme 2

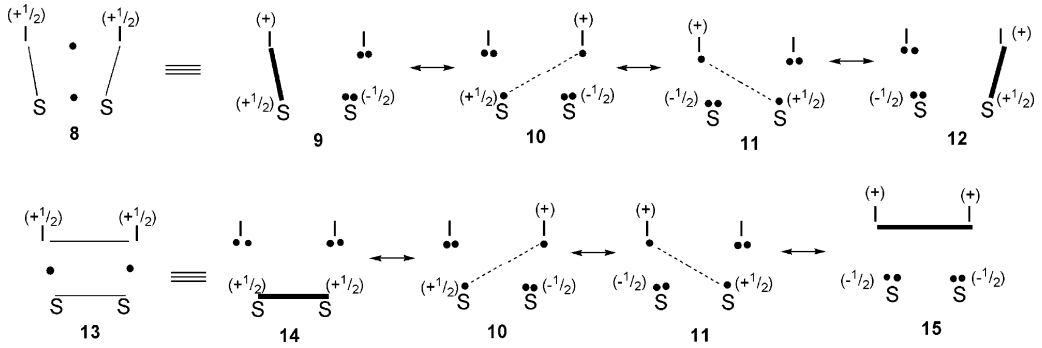

Scheme 3

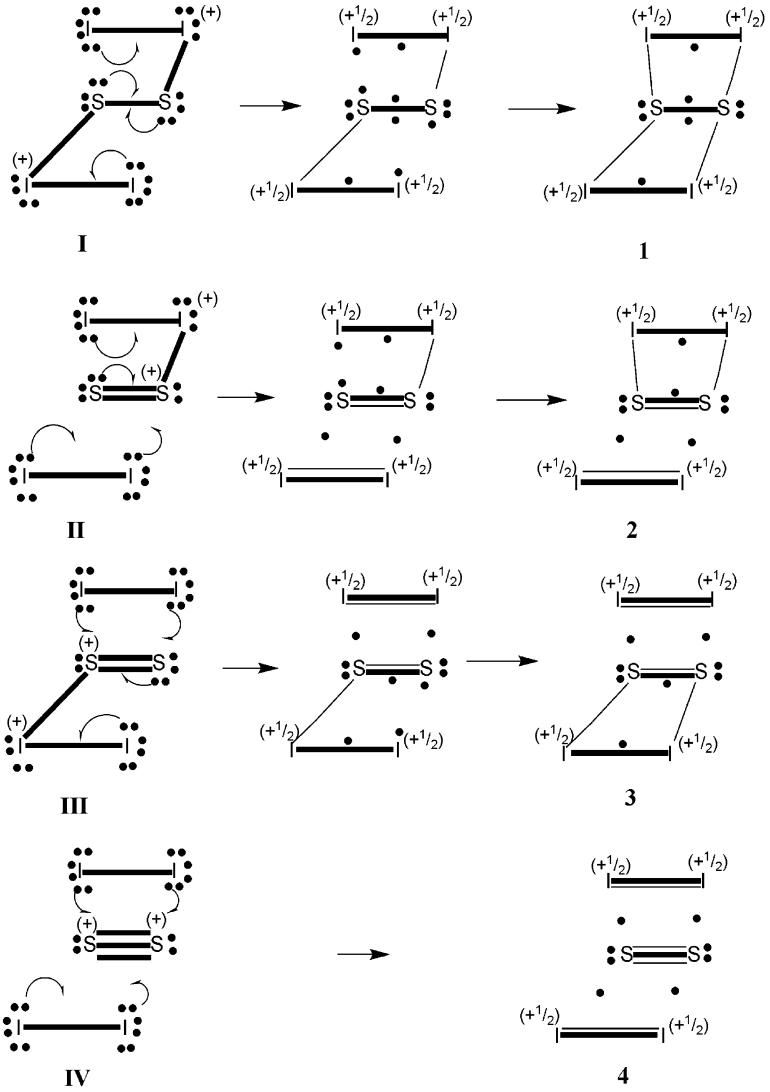

A VB description for $S_2Cl_4^{2+}$, which has been used as a model for $Se_2I_4^{2+}$, has been provided in ref 17a. $S_2O_4^{2-}$ also has a similar type of electronic structure to $Se_2I_4^{2+}$, as both have a long E−E bond (E = Se, S).[16,17]

3.2.4. NBO Analysis. An NBO analysis was performed on **A**, **B**, **D1**, and **D2** conformations of $S_2I_4^{2+}$ and $Se_2I_4^{2+}$ ions and indicated strongly delocalized bonding situations in all cases.

3.2.4.1. A-$S_2I_4^{2+}$ (A-$Se_2I_4^{2+}$). The NBO representation of **A** structures is achieved by starting from closed-shell species S_2^{2+} (Se_2^{2+}) and two I_2, with transfer of p^2 electrons on adjacent iodine atoms into antibonding S_2^{2+} (Se_2^{2+}) orbitals

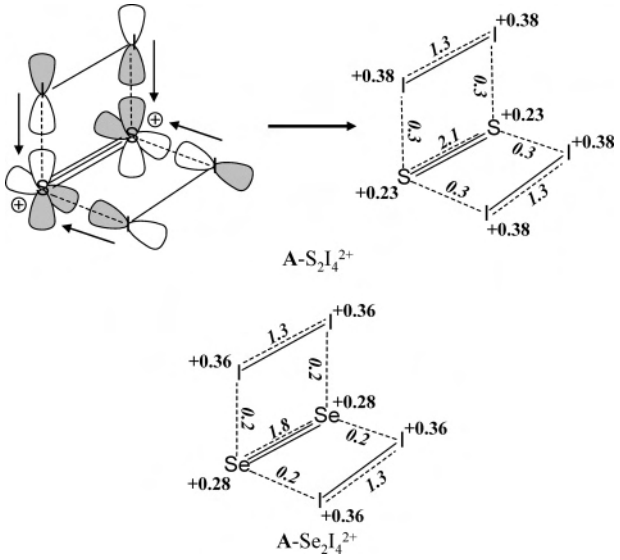

Figure 14. Charge transfer from diiodine p^2 orbitals into S_2^{2+} π^* orbitals and relative Mayer bond orders (bold italic) and natural charges (bold) of **A**-$S_2I_4^{2+}$ and **A**-$Se_2I_4^{2+}$.

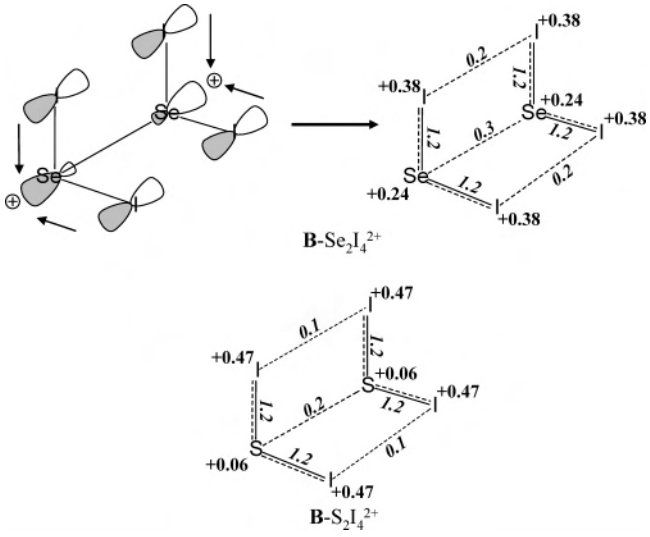

Figure 15. Charge transfer from iodine p^2 orbitals into the Se−Se σ^* orbital and relative Mayer bond orders (bold italic) and natural charges (bold) of **B**-$Se_2I_4^{2+}$ and **B**-$S_2I_4^{2+}$. For comparison, the Se−I relative Mayer bond order and the Se natural charge in SeI_2^+ are 1.2 and 0.30, respectively.

accompanied by an energy stabilization, as shown in Figure 14. This reduces the charge on S_2^{2+} (Se_2^{2+}) from 2 to 0.46 (0.52) in **A**-$S_2I_4^{2+}$ (**A**-$Se_2I_4^{2+}$) with a corresponding decrease in bond order from 3 to 2.1 (1.8). The charge on I_2 increases to 0.76 (0.72), and the bond order increases to 1.3 (1.3). The NBO bond orders seem to be slightly smaller than those predicted by the simple bonding model but are comparable with those obtained by the AIM analysis (see Figure 5). In line with the AIM results, the NBO analysis places more of the positive charge on iodine atoms than on sulfur atoms. Apart from the atomic charges, the final NBO bonding description illustrated in Figure 14 for **A**-$S_2I_4^{2+}$ (**A**-$Se_2I_4^{2+}$) is in excellent agreement with the simple bonding model (see Figure 1).

3.2.4.2. B-$Se_2I_4^{2+}$ (B-$S_2I_4^{2+}$). The classical all-σ-bonded structure is the parent Lewis structure for **B**-$Se_2I_4^{2+}$ (**B**-$S_2I_4^{2+}$). The **B**-$Se_2I_4^{2+}$ structure is obtained by charge (electron) transfer from the iodine p lone pair orbitals to the Se−Se σ^*-antibonding NBO, as illustrated in Figure 15. The charge transfer decreases the positive charge on selenium (sulfur) atoms from +1 to +0.24 (+0.06) and thus lowers the energy of the **B** structure. The occupation of σ^*-antibonding NBO decreases the Se−Se (S−S) bond order from 1 in the parent Lewis structure to the observed 0.3 (0.2). The accompanying depletion of p^2 electrons that are σ^*-antibonding with respect to the I−I contacts results in a weak bonding interaction between iodine atoms with a bond order of 0.2 (0.1). Thus, the bonding between SeI_2^+ units can be described by a delocalized 6c2e bond in accordance with the FMO description.

In accordance with AIM results, the NBO analysis predicts minor changes in SeI_2^+ units (Se−I bond order 1.2 and Se natural charge +0.30) upon dimerization, largest of which is the charge transfer from selenium to iodines in **B**-$Se_2I_4^{2+}$. Thus it can be concluded that, even though the charge distribution and delocalization given by the simple bond model is an oversimplification of the total bonding situation,

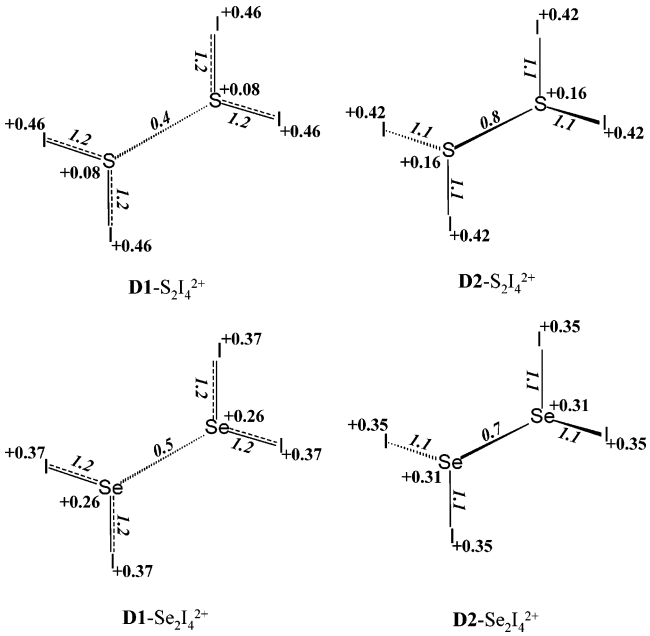

Figure 16. Relative Mayer bond orders (bold italic) and charges (bold) of **D1**-$S_2I_4^{2+}$, **D2**-$S_2I_4^{2+}$, **D1**-$Se_2I_4^{2+}$, and **D2**-$Se_2I_4^{2+}$.

qualitatively the simple bonding model works surprisingly well for **A**-$S_2I_4^{2+}$ and **B**-$Se_2I_4^{2+}$.

3.2.4.3. D Structures. The classical all-σ-bonded structure is also the parent Lewis structure for the **D1** and **D2** structures that are presented in Figure 16. Similar charge (electron) transfer from iodine p^2 orbitals to the E−E σ^* antibonding NBO as in the **B** structures is observed in **D1** and **D2** structures. The energy gain by relieving the repulsion between the positively charged chalcogen atoms, even in the approximately singly bonded **D2** structures, results in a partly nonclassical bonding situation, as manifested by the chalcogen−chalcogen bond orders and atomic charges. The charge transfer is greater in the structures of $S_2I_4^{2+}$ than in the respective structures of $Se_2I_4^{2+}$, which causes the Se−Se bond order to be higher than that of the S−S bond in the

Table 6. Born−Haber Cycle for the Stepwise Isomerization (Energies in kJ/mol) from **A** to **B** Structure[a]

	$Se_2I_4^{2+}$	$S_2I_4^{2+}$	$S_2Br_4^{2+}$	$S_2Cl_4^{2+}$	$I_2SeSI_2^{2+}$	$Te_2I_4^{2+}$
(i) **A**-$E_2X_4^{2+} \rightarrow E_2^+ + X_2 + X_2^+$	−62.7	−74.4	−129.9	−164.9	−70.6	−57.6
(ii) $E_2^+ \rightarrow E_2 - e^{-b}$	−857.7	−896.3	−896.3	−896.3	−873.3	−787.5
(iii) $X_2 + X_2^+ \rightarrow 2X_2 - e^{-b}$	−917.5 [c]	−917.5 [c]	−1015.9	−1100.4	−917.5 [c]	−917.5 [c]
(iv) $E_2 \rightarrow 2E$	+314.4	+389.3	+389.3	+389.3	+348.4	+264.3
(v) $2X_2 \rightarrow 4X$	+332.3	+332.3	+390.2	+434.9	+332.3	+332.3
(vi) $2E + 4X \rightarrow 2EX_2$	−728.5	−743.2	−848.2	−965.0	(−364.3) (SeI_2) + (−371.6) (SI_2)	−729.7
(vii) $2EX_2 - 2e^- \rightarrow 2EX_2^+$	+1645.6	+1683.6	+1769.3	+1818.3	+822.8 (SeI_2) +841.8 (SI_2)	+1762.1
(viii) $2EX_2^+ \rightarrow$ **B**-$E_2X_4^{2+}$	+229.5	+242.8	+283.4	+316.0	+235.7	+17.9

[a] Absolute calculated energies and geometries are given in the Supporting Information. [b] For comparison, experimental ionization energies (kJ/mol) are S_2, 903 ± 1; Se_2, 860 ± 20; Te_2, 794 ± 3; SeS, 890 ± 20; Cl_2, 1108 ± 1; Br_2, 1015 ± 1; I_2, 898 ± 1.[2,69] [c] The relatively large difference between experimental and calculated IE of I_2 is related to spin−orbit coupling, which is not accounted for by the calculation.[70]

B, **D1**, and **D2** structures. The NBO analysis establishes the role of positive charge delocalization (transfer) as one of the driving forces leading to the nonclassical structures of these cations in accordance with the previous suggestions.[15,22]

3.2.5. ELF Analysis. In addition to the methods presented above, electron localization function (ELF) analysis[65] was also used to study the bonding in $S_2I_4^{2+}$ and $Se_2I_4^{2+}$ structures. However, because the ELF results simply confirmed the conclusions made with other methods and because of the difficulties encountered in relating the bond basin populations to bond orders, the ELF results are presented in detail in the Supporting Information.

3.3. Accounting for the Differences in the Structures of A-$S_2I_4^{2+}$, B-$Se_2I_4^{2+}$, and P_2I_4 (As_2I_4). The calculations correctly reflect the experimental findings that for $S_2I_4^{2+}$ the **A** structure is lower in energy than the **B** structure and that the reverse is true for $Se_2I_4^{2+}$ (see Figure 3). In addition, the π-bonded **A** and **B** structures are lower in energy than the **D2** structures, which approximate the experimental structures of the isoelectronic σ-bonded P_2I_4 and As_2I_4.

The AIM and NBO analyses have already inferred the role of charge delocalization as one of the driving forces that lead the $S_2I_4^{2+}$ and $Se_2I_4^{2+}$ to adopt their nonclassical structures. In this section we point out other factors that lead to the observed energy differences between the **A**, **B**, and **D2** structures by first giving a semiquantitative description of the differences and then attempting a quantitative analysis.

3.3.1. "Back of the Envelope" Qualitative Approach. The different stabilities of **A** and **B** structures for $S_2I_4^{2+}$ and $Se_2I_4^{2+}$ ions have been attributed to weaker π-bonding on Se_2 relative to S_2 and the similar ionization energies of S_2(g) and I_2(g).[5e,14,22] The effect of different π-bond strengths (see Table 1) to the relative stabilities of **A** and **B** structures can be evaluated very roughly by approximating the **A** conformation as having one E═E double bond and two I−I single bonds and the **B** conformation as having four E−I single bonds. In addition, both conformations are expected to have further small π-bonding contributions that sum up to a single π bond, which we assume to have approximately the same contribution to the total bond energy in both conformations. Summing the bond energies, the **B** conformations are predicted to be more stable than the **A** structures by 13 kJ/mol for $S_2I_4^{2+}$ and 74 kJ/mol for $Se_2I_4^{2+}$.[66,67]

The E−I (E = S, Se) bond energies are similar and small (see Table 6), a consequence of the near equality of the electronegativities of I, S, and Se, and the reason for the instability of neutral binary sulfur and selenium iodides and covalent S−I and Se−I bonds.[18a] However, the S═S bond dissociation energy is significantly greater than that of Se═Se (see Table 1), accounting for the greater stability of the **A** isomer for $S_2I_4^{2+}$ relative to the case for $Se_2I_4^{2+}$. The difference between the relative energies based on this simple approach and the values obtained by DFT calculations (see Figure 3) are related to the unaccounted π-bonding contributions and the stabilizing effect of charge delocalization. Thus, on the basis of this simple bonding model, the small increase of charge delocalization that was observed in AIM and NBO analyses in going from **B** conformation to **A** conformation in $Se_2I_4^{2+}$ does not seem to be enough to compensate for the bond energy differences of the two structures, whereas the larger increase of charge delocalization in $S_2I_4^{2+}$ is enough to tip the stabilities of **A** and **B** structures in favor of the **A** structure.

The relative stabilities of **B** structures compared to the classical structures can be evaluated in a similar way to the above treatment of **A** and **B** structures. The classical structure of $E_2I_4^{2+}$ (E = S, Se) has four E−I σ bonds and one E−E σ bond and the **B** structure has four E−I σ bonds, one delocalized E−I π bond, and the π*−π* bonds. If charge delocalization is disregarded, the energy difference between these structures is determined by the relative energies of the E−E σ bond (E = S, Se) compared to the delocalized E−I π bond (one over the whole $E_2I_4^{2+}$) and the π*−π* bond (σ(S−S) 226 kJ/mol vs π(S−I) 148 kJ/mol and σ(Se−Se) 172 kJ/mol vs π(Se−I) 106 kJ/mol).[68] Comparison of the

(65) (a) Becke, A. D.; Edgecombe, K. E. *J. Chem. Phys.* **1990**, *92*, 5397. (b) Silvi, B.; Savin, A. *Nature* **1994**, *371*, 683.

(66) Pauling, L. *The Nature of the Chemical Bond*, 3rd ed.; Cornell University: Ithaca, NY, 1960.

(67) The E−I σ-bond energies are estimated using Pauling's equation for heteroatomic bond strengths: $D_{A-B} = (D_{A-A}D_{B-B})^{1/2} + 96.5(X_A - X_B)^2$, where D_{A-A} is the homoatomic single-bond energy and X_A is the electronegativity of atom A.[66] Equation gives D_{S-I}/[kJ/mol] = $(226\times149)^{1/2} + 96.5(2.58 - 2.66)^2 = 184$ and D_{Se-I}/[kJ/mol] = $(172\times149)^{1/2} + 96.5(2.55 - 2.66)^2 = 161$. The energy differences between **A** and **B** structures are $\Delta E(S_2I_4^{2+})$/[kJ/mol] = $(425 + 2\times49) - (4\times184) = -13$ and $\Delta E(Se_2I_4^{2+})$/[kJ/mol] = $(272 + 2\times149) - (4\times161) = -74$.

(68) The E−I π-bond energies are estimated in a similar fashion to σ-bond energies.[67] No I−I π-bond energy has been reported, and therefore, the I−I π-bond energy is estimated by assuming that the π/σ bond energy ratio is the same as for the tellurium bonds. Estimated I−I π-bond energy is 110 kJ/mol. The E−I π-bond energies are $D(\pi)_{S-I}$/[kJ/mol] = $(199\times109)^{1/2} + 96.5(2.58 - 2.66)^2 = 148$ and $D(\pi)_{Se-I}$/[kJ/mol] = $(100\times109)^{1/2} + 96.5(2.55 - 2.66)^2 = 106$.

Scheme 4. Born−Haber Cycle for the Isomerization Reaction from **A** Structure to **B** Structure

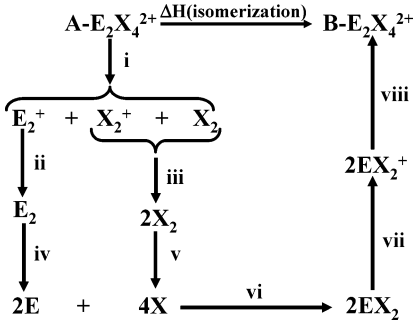

relative stabilities of σ and π bonds clearly indicates that the classical structure should be favored. However, the lengthening of the $^{+}I_2E\cdots EI_2^{+}$ bond (E = S, Se) going from the **D2** structure to **D1** structure lowers the energy by 16.0 (S) and 16.2 (Se) kJ/mol (see Figure 3) with only slight changes in atomic charges (see Figures 10 and 16). Thus the loss in E−E σ-bond energy is more than compensated by the gain in E−I π bonding and the lowering of electrostatic repulsion between EI_2^{+} units. The smaller energy differences between **D1**, **C**, and **B** structures are attributed to the further gain in E−I π bonding and $\pi^*-\pi^*$ bonding. Thus, from this approach we can conclude that the electrostatic repulsion between EI_2^{+} units is a major reason why the nonclassical structures are adopted by $S_2I_4^{2+}$ (**A**) and $Se_2I_4^{2+}$ (**B**). The minimization of the repulsion between EI_2^{+} units in **D2** by positive charge delocalization from E to I is also the major reason why even the **D2** structure does not adopt the classical bonding, as shown by the NBO analysis. In contrast, there is no charge delocalization required in the neutral P_2I_4 (As_2I_4) molecules and they readily adopt the classically σ-bonded structures.

3.3.2. Born−Haber Quantitative Approach. A more quantitative approach to the different stabilities of **A** and **B** conformations of $S_2I_4^{2+}$ and $Se_2I_4^{2+}$ is given by breaking the isomerization process into steps by using a Born−Haber cycle (Scheme 4). The calculated energies of the separate reaction steps are given in Table 6. The energy changes of all reactions are in general higher for $S_2I_4^{2+}$ than for $Se_2I_4^{2+}$. The reactions are divided into three classes (**a**) the breaking and forming of weak $\pi^*-\pi^*$ bonds in $E_2X_4^{2+}$ cations (reactions **i** and **viii**), (**b**) ionization of E_2, X_2, and EX_2 molecules (reactions **ii**, **iii**, and **vii**), and (**c**) breaking of strong dichalcogen and dihalogen bonds and forming of chalcogen−halogen bonds (reactions **iv**, **v**, and **vi**). The energy losses/gains for the different classes of reactions are presented in Table 7.

(**a**) Both experimental structures of the dications $S_2I_4^{2+}$ and $Se_2I_4^{2+}$ are thermodynamically unstable toward the breaking of the weak $\pi^*-\pi^*$ bonds with dissociation into monocations (Table 6, **i** and **viii**) in the gas phase showing that their structures are lattice stabilized in the solid state.[11] **A** isomers of both cations are more stable toward dissociation into monocations than **B** isomers, and thus, the dissociations favor the **A** structures with an almost equal energy change for both $S_2I_4^{2+}$ and $Se_2I_4^{2+}$.

(**b**) There is more energy gained from the deionization of dichalcogens and diiodine (**ii** and **iii**) than lost in the ionization of chalcogendiiodine molecules (**vii**). Therefore, the ionization reactions favor the formation of **B** structures. The total energy change for **b** reactions is almost the same for both cations (see **b** in Table 7).

(**c**) The breaking of dichalcogen (**iv**) and diiodine (**v**) bonds requires less energy than is gained in the formation of chalcogen−iodine (**vi**) bonds and thus favors the formation of **B** structures (see **c** in Table 7). The energy change for **c** reactions is larger by 60.2 kJ/mol for $Se_2I_4^{2+}$ than it is for $S_2I_4^{2+}$, while the energy changes for **a** and **b** reactions are almost equal (see above). It has to be noted that this value is almost identical to the total energy difference (ΔE(**A** → **B**)) of **A** and **B** structures in $S_2I_4^{2+}$ and $Se_2I_4^{2+}$ (61.3 kJ/mol). Therefore, it can be concluded that the different stabilities of homoatomic bonds compared to chalcogen−iodine bonds (**c** reactions) account for most of the difference in stabilities of **A** and **B** structures of $S_2I_4^{2+}$ and $Se_2I_4^{2+}$. The difference in ionization energy of Se_2 compared to S_2 and I_2 seems to play only a minor role, contrary to our previous suggestion.[15] The strength of the S_2 bond drives $S_2I_4^{2+}$ to the **A** structure.

3.3.3. The Nonexistent $I_2SeSI_2^{2+}$, $S_2Cl_4^{2+}$, $S_2Br_4^{2+}$, and $Te_2I_4^{2+}$ Species and the Uniqueness of A-$S_2I_4^{2+}$. The steps in the Born−Haber cycle (Scheme 4) for the isomerization from **A** to **B** structures were also determined for $I_2SeSI_2^{2+}$, $S_2Cl_4^{2+}$, $S_2Br_4^{2+}$, and $Te_2I_4^{2+}$ cations in order to study the possibility of synthesizing related chalcogen−halogen cations (Tables 6 and 7). All cations favor the formation of the **B** structure, with the exception of $S_2I_4^{2+}$. This underlines the extraordinary nature of $S_2I_4^{2+}$ compared to other $E_2X_4^{2+}$-type species, which arises from the relative strengths of homoatomic multiple bonds compared to chalcogen−halogen single bonds (see Table 1).

The relative stability of the **B** isomer of $S_2X_4^{2+}$ increases as I → Br → Cl. **A**-$S_2I_4^{2+}$ is more stable than **B**-$S_2I_4^{2+}$, but the reverse is true for $S_2Br_4^{2+}$ and $S_2Cl_4^{2+}$. $Te_2I_4^{2+}$ seems to behave somewhat differently from the other cations. In contrast to the other cations, the calculated dissociation into monocations supports the formation of the **B** isomer and the ionization processes the formation of the **A** isomer. However, the relatively strong Te−I bond tips the balance clearly to the **B** structure, and **B**-$Te_2I_4^{2+}$ salts seem viable candidates for synthesis provided that disproportionation reactions do not lead to more stable products.

3.4. Comparison of the S−S Bond Orders in A-$S_2I_4^{2+}$ and Other Highly π-Bonded Compounds of Heavier Main Group Elements. The bond orders for **A**-$S_2I_4^{2+}$ that have been determined by different methods are gathered in Table 8. It has been shown that the S−S bond in $S_2I_4^{2+}$ has an experimental bond order of 2.2−2.4,[11] while the theoretical normalized bond orders are predicted to be 1.6−2.3 depending on the method used.

The range of normalized theoretical bond orders for the S−S bond in **A**-$S_2I_4^{2+}$ is rather large. The AIM delocalization indices are the lowest and deviate greatest from the other values. It is expected that the normalization of the delocal-

Table 7. Energy Changes [kJ/mol] Divided into Different Classes of Reactions in the Born−Haber Cycle for the Isomerization from **A** to **B** Structure

	$Se_2I_4^{2+}$	$S_2I_4^{2+}$	$S_2Br_4^{2+}$	$S_2Cl_4^{2+}$	$I_2SeSI_2^{2+}$	$Te_2I_4^{2+}$
a (i + viii)	+166.8	+168.0	+153.5	+151.1	+167.5	−39.7
b (ii + iii + vii)	−129.6	−130.2	−142.9	−177.9	−126.2	+57.1
c (iv + v + vi)	−81.8	−21.6	−68.7	−140.8	−55.2	−133.1
∑ (a,b,c) = Δ*E* (A → B)	−44.6	+16.6	−58.1	−168.1	−16.3	−115.7

Table 8. Relative Bond Order Estimates for $S_2I_4^{2+}$ and Other Species with High Bond Orders[a]

	theoretical based BOs			experiment based BOs		
	ρ_{BCP}	**δ(A,B)**	Mayer[b]	Pauling[c]	*X*−*X* stretching frequency[c]	normal coordinate analysis[c]
				S−S Bonds		
A-$S_2I_4^{2+}$	2.3	1.6	2.1	2.4[d]/2.7[e]	2.2	2.2
S═S═O[h]	2.1	1.5	2.1	2.1	1.9	2.0
S═SF_2[h]	2.1	1.5	2.2	2.3	2.3	2.1
F−S−S−F[h]	2.0	1.2	2.0	2.1	1.5	1.4
				I−I Bonds		
A-$S_2I_4^{2+}$	1.5	1.1	1.3	1.3	1.3	1.3
I_2^+	1.5	1.5	1.4			
I_4^{2+}	1.5 / 0.2	1.2/0.2	1.5/0.3			
				Si−Si Bonds		
bent $Si_2(SiH_3)_2$	2.1	2.7	2.7	2.4[f]/2.5[g]		

[a] The determination of the relative bond orders has been described in the Supporting Information. [b] See ref 71. [c] See ref 11. [d] AsF_6^- salt. [e] SbF_6^- salt. [f] See ref 72. [g] Calculated for the experimental bond length found in the compound by Sekiguchi et al.[8] [h] Increased-valence structures with 2c1e bonds are displayed in ref 16 for SSO, FSSF, and SSF_2.

ization index is compromised because the normalization is done with comparison to a series of diatomic species S_2^n (n = 1−, 0, 1+, 2+), and delocalization indices are known to depend on the number of other bonds on the atom in question.[30a] Similarly, the I−I bonds in $S_2I_4^{2+}$ are predicted to have lower bond orders, based on delocalization indices, than with other methods when compared to I_2 and I_2^+. If the AIM delocalization index results are omitted, the S−S theory-based bond order values are close to 2.2, which is in good agreement with bond orders calculated from experimental results[11] and the approximate bond order estimate from the molecular orbital analysis (see Section 3.2.2.1).

Comparison with other sulfur molecules, which are expected to have high bond orders (see Table 8), indicates that **A**-$S_2I_4^{2+}$ has a significantly higher S−S bond order than F−S−S−F and S═S═O. On the other hand, comparison with S═SF_2 produces mixed results, and it can only be concluded that the S−S bond orders of **A**-$S_2I_4^{2+}$ and S═SF_2 are so alike that the accuracy of the methods is not enough to tell them apart. A similar conclusion was drawn from the experimental results.[11]

A straightforward way to compare the apparently high S−S bond order in $S_2I_4^{2+}$ with that of homoatomic multiple bonds between other heavier main group elements is by comparison to the bent Si−Si triple-bonded $[(Me_3Si)_2CH]_2$-(^{i}Pr)SiSi≡SiSi(^{i}Pr)$[CH(SiMe_3)_2]_2$ (Si−Si 2.0622(9) Å).[8] Due to the large computational effort associated with calculating the structure of $[(Me_3Si)_2CH]_2(^iPr)SiSi{\equiv}SiSi(^iPr)[CH(SiMe_3)_2]_2$, previous studies have used the bent structures of Si_2R_2 (R = H, Me, Ph, and SiH_3) as models for the Si−Si "triple bond". The calculated bond orders varied from 2.0 to 2.8 depending on the method used in the calculation.[8,9a−d] The orbital-based methods usually resulted in higher bond orders, while the topological methods predicted bond orders closer to 2. The studies, which have yielded the high bond orders using orbital-based methods, have been criticized in that they assign orbitals with significant nonbonding character as purely bonding orbitals, thus resulting in bond orders that are too high.[9a,d,h] On the other hand, those employing the orbital-based methods have argued that the discrepancy between bond orders from topological and orbital-based methods arises from the different and weaker nature of the bonds in bent structures compared to the bonds in acetylene but that qualitatively the number of bonds between silicon atoms is three and not two as the topological methods have indicated.[9j]

Following the example of the most recent topological paper on the subject, we have chosen the bent $Si_2(SiH_3)_2$ as a model for the Si−Si "triple bond".[9d] The relative Si−Si bond orders varied from 2.1 to 2.7 depending on the method used (see Table 8). The smallest Si−Si bond order was predicted from the AIM critical point density and the highest with the Mayer bond index in accordance with previous findings.[8,9a−d] It has to be noted that the delocalization index also predicted a high Si−Si bond order of 2.7 in contrast to the recent findings of Pignedoli et al.[9d] who predicted a Si−Si bond order of 2.15 using a similar renormalized AIM bond order method. The Pauling bond order for the bent Si−Si bond (2.4 for calculated/2.5 for experimental bond length) was determined to be similar to that of the S−S bond in $S_2I_4^{2+}$. In conclusion, the nonsterically hindered **A**-$S_2I_4^{2+}$ seems to have either a similar or a slightly smaller S−S bond order than the Si−Si bond order in the bent silicon model structure and the proposed sterically protected triply bonded silicon compound depending on the method that is used to determine the bond orders.

The overall picture of bond orders produced by the different methods is not very consistent, reflecting the difficulties and uncertainties found in all bond-order calculations. The bond order estimates vary considerably from bond to bond depending on the method used. This is related to the fact that the methods do not actually calculate the bond order itself but rather something else that has been associated with the bond order. However, there is no generally accepted

agreement on which method is the best for assigning bond orders. We have used several methods in combination with chemical knowledge to determine which give reasonable results on a case-by-case basis.

4. Conclusions

The bonding of $S_2I_4^{2+}$, $Se_2I_4^{2+}$, and their higher-energy isomers have been investigated by modern DFT and ab initio calculations and theoretical analysis methods, AIM and NBO analyses, as well as MO and VB theories. The aim of the paper was to seek answers to four main questions: (1) Are the previously proposed simple bonding models (see Figures 1 and 2) valid for $S_2I_4^{2+}$ and $Se_2I_4^{2+}$? (2) What accounts for the difference in the structures of $S_2I_4^{2+}$ and $Se_2I_4^{2+}$? (3) Why are the classically bonded isolobal P_2I_4- and As_2I_4-type structures not adopted by $S_2I_4^{2+}$ and $Se_2I_4^{2+}$? (4) Is the high experimentally observed S−S bond order in $S_2I_4^{2+}$ supported by theoretical bond orders, and how does it relate to the high homoatomic bond orders between other heavier main group elements?

4.1. Bonding in $S_2I_4^{2+}$ and $Se_2I_4^{2+}$. The simple bonding models derived from frontier molecular orbital theory were shown to be qualitatively correct for both $S_2I_4^{2+}$ (see Figure 1) and $Se_2I_4^{2+}$ (see Figure 2). The AIM analysis showed the weak bonds in $S_2I_4^{2+}$ and $Se_2I_4^{2+}$ to be real and the bonding in these cations to be covalent in nature. The theoretical bond orders for $S_2I_4^{2+}$ from AIM, NBO, and full MO analyses agreed well with the bond orders predicted by the simple bonding model (see Figure 1). The full MO analysis confirmed that the bonding between S_2 and two I_2^+ units in $S_2I_4^{2+}$ is described by two mutually perpendicular 4c2e $\pi^*-\pi^*$ bonds and that the simple bonding model includes all the major aspects of bonding found by the full analysis. The only large difference between the simple bonding model and AIM and NBO results is the charge distribution. While the simple model predicts equal charge distribution over $S_2I_4^{2+}$, AIM and NBO analyses show that the positive charge is, rather surprisingly, more localized on the iodine atoms.

The AIM, NBO, and full MO analyses for $Se_2I_4^{2+}$ showed only small differences with the simple bonding model (see Figure 2). In the AIM and NBO analyses, the SeI_2^+ units in $Se_2I_4^{2+}$ do not stay as unchanged upon dimerization as in the simple bonding model. The major change is that there is some positive charge transfer from selenium to iodine atoms in $Se_2I_4^{2+}$ (i.e., electron transfer from iodine to selenium). The bond orders from AIM and NBO analyses on the other hand were within the accuracy of the bond-order determination compared to the simple model, e.g., BO (SeI) = $1^1/_4$. The full MO analysis showed that qualitatively the 6c2e intradimer $\pi^*-\pi^*$ bond suggested by the simple bonding model does describe the bonding in $Se_2I_4^{2+}$ but that for a quantitative description the small contributions to bonding from lower valence orbitals must be included. However, as quantification of these small contributions proved to be difficult within the MO approach, the simple FMO bonding model can be considered as satisfactorily describing the bonding in $S_2I_4^{2+}$ and $Se_2I_4^{2+}$. This work provides further support for the applicability of the simple bonding models and their concepts of charge delocalization, $np_\pi-np_\pi$ ($n \geq 3$), $p^2 \rightarrow \sigma^*$, and $\pi^*-\pi^*$ bonding to describe the bonding in the other species of electron rich elements, many of which adopt nonclassical and clusterlike structures.[18,20] Previous theoretical calculations on E_4^{2+} [54] and E_8^{2+} (E = S, Se)[18d] also provided justification for these simple bonding models.

A complementary qualitative approach to the MO treatment in describing the bonding of $S_2I_4^{2+}$ was provided by the VB approach. The VB approach gives resonance structures to describe the bonding, given the input of bond orders and charge distribution. To the first approximation, the bonding in $S_2I_4^{2+}$ is described by resonance between the increased-valence structures **1**−**3** (see Scheme 1), the VB equivalent of the simple FMO model shown in Figure 1. The increased-valence structure **1** involves the covalent component of the 4c2e $\pi^*-\pi^*$ bonding scheme for each of the two mutually perpendicular 4c2e $\pi^*-\pi^*$ bonds.

4.2. Reasons for the Difference in the Structures of $S_2I_4^{2+}$ and $Se_2I_4^{2+}$. The calculations confirmed (see Figure 3) that the different structures adopted by $S_2I_4^{2+}$ (**A**) and $Se_2I_4^{2+}$ (**B**) are intrinsic to these cations and not just caused by solid-state effects. Contrary to our previous suggestion,[22] the difference in ionization energy of Se_2 compared to S_2 and I_2 plays only a minor role in the different stabilities of the **A** and the **B** structures of $S_2I_4^{2+}$ and $Se_2I_4^{2+}$. A Born−Haber cycle written for the isomerization process from the **A** to the **B** structure (see Scheme 4) showed clearly that the major reason why $S_2I_4^{2+}$ and $Se_2I_4^{2+}$ adopt different structures is the high π-bond strength of S_2 (and the S−S bond in the **A** structure of $S_2I_4^{2+}$) relative to the weak σ S−I bonds (in the **B** structure) (see Table 1). The several examples of stable compounds containing S−S $p_\pi-p_\pi$ bonds, as well as the paucity of such examples for nonsterically protected situations for the heavier elements of the earlier rows of the periodic table, can be accounted for in part by the higher π/σ homoatomic bond energy ratio for sulfur (see Table 1). A small stabilizing contribution comes from the increased delocalization of positive charge in the **A** structure of $S_2I_4^{2+}$ compared to the **B** structure, while the positive charge is sufficiently delocalized in all structures of $Se_2I_4^{2+}$ and thus does not affect, to the same extent, the different stabilities of the structures of $Se_2I_4^{2+}$.

A comparison with other $E_2X_4^{2+}$-type ions (E = S, Se, Te; X = Cl, Br, I) indicated that $S_2I_4^{2+}$ is the lone exception in exhibiting the highly homoatomic π-bonded **A** structure, as all other calculated chalcogen−halogen cations favored the observed structure of $Se_2I_4^{2+}$ (**B**).

4.3. Why Are Classical Structures Not Adopted by $S_2I_4^{2+}$ and $Se_2I_4^{2+}$? The minimization of the electrostatic repulsion between EI_2^+ units is concluded to be the major driving force for $Se_2I_4^{2+}$, as well as $S_2I_4^{2+}$, to adopt their nonclassical structures (see Figure 3). Polyatomic dications are thermodynamically unstable in the gas phase toward dissociation into separated monocations due to the electrostatic repulsion between charges.[10i] For $S_2I_4^{2+}$ the energy required to adopt the **B** structure (16.0 kJ/mol) is significantly less than that required to go from $S_2I_4^{2+}$ (**B**) to that of **D2** (31.1 kJ/mol). Comparing the $Se_2I_4^{2+}$ (**B**) structure to the

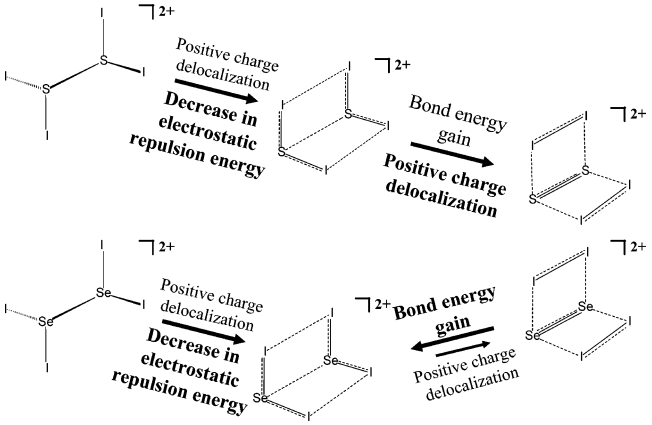

Figure 17. Summary of the factors causing $S_2I_4^{2+}$ and $Se_2I_4^{2+}$ to adopt their observed structures.

approximately singly bonded structure (**D2**) shows that the loss in E−E σ-bond energy is more than compensated by the gain in E−I π bonding, $\pi^*-\pi^*$ bonding, and the lowering of the electrostatic repulsion between EI_2^+ units. NBO results show that nonclassical bonding is even adopted by the **D2** structure to maximize positive charge delocalization. The factors causing $S_2I_4^{2+}$ and $Se_2I_4^{2+}$ to adopt their experimentally observed structures have been summarized in Figure 17. In contrast, no charge delocalization is required in the neutral P_2I_4 and As_2I_4 molecules and they readily assume the classically σ-bonded structures. The nonclassically bonded structures of many other main group dications, e.g., I_4^{2+}, E_4^{2+} (E = S, Se, Te), and E_8^{2+} (E = S, Se)[18,20] is also the result of similar minimization of positive charge repulsion by charge delocalization in their hypothetical σ-bonded isomers.

4.4. High S−S Bond Order in $S_2I_4^{2+}$. Theoretical bond orders calculated in this paper confirm the experimental evidence presented previously for the high S−S and I−I bond orders in $S_2I_4^{2+}$ cation,[11] and we conclude that the S−S and I−I bond orders are close to 2.2 and 1.4, respectively. The comparison with other multiply bonded sulfur species indicates that $S_2I_4^{2+}$ cation ties with S=SF_2[73] for first place for having the highest reported S−S bond order. The comparison to the bent $Si_2(SiH_3)_2$ structure, which is used as a model for the triply bonded structure of Sekiguchi et al.,[8] concludes that the S−S bond order in $S_2I_4^{2+}$ is either similar to or slightly less than the Si−Si bond order for $[(Me_3Si)_2CH]_2$-(^{i}Pr)SiSi≡SiSi(^{i}Pr)$[CH(SiMe_3)_2]_2$ depending on the method used for determining the bond orders. These results provide further evidence that the heavier elements of Groups 13, 14, and 15 are not the only ones that have high and interesting multiple bonding between $n \geq 3$ elements. We hope that these results will help to enlarge discussions of multiple bonding between the heavier main group elements to include the long known and well established examples from Groups 16 and 17 which, with few exceptions, have been overlooked.

Acknowledgment. We thank the Natural Sciences and Engineering Research Council (NSERC) of Canada for funding (J.P.) and a Graduate Scholarship (S.B.), the Alexander von Humboldt Foundation in Germany for providing two Feodor−Lynen Fellowships (M.-J.C., C.K.), the Academy of Finland (R.S.L.), the Ministry of Education in Finland, and the Helsingin Sanomain 100-vuotissäätiö for providing partial financial support (J.M.R.), and Dr. Fritz Grein for valuable discussions over many years.

Supporting Information Available: Calculated absolute energies and structural parameters; discussion of basis set and method dependence of the relative energies; discussion of estimation of relative weights for the increased valence structures; discussion of ELF analyses; NBO results; description of the normalization procedures used for determination of the Pauling bond orders and the theoretical bond orders. This material is available free of charge via the Internet at http://pubs.acs.org.

IC061523W

(69) (a) Grade, M.; Wienecke, J.; Rosinger, W.; Hirschwald, W. *Ber. Bunsen-Ges. Phys. Chem.* **1983**, *87*, 355. (b) Potts, A.W.; Novak, I. *J. Electron Spectrosc. Relat. Phenom.* **1983**, *28*, 267.

(70) Frost, D. C.; McDowell, C. A.; Vroom, D. A. *J. Chem. Phys.* **1967**, *46*, 4255.

(71) (a) Mayer, I. *Chem. Phys. Lett.* **1983**, *97*, 270. (b) Mayer, I. *Int. J. Quantum Chem.* **1984**, *26*, 151.

(72) The BO was calculated using a modified Pauling formula $D_n = 2.361 - 0.728 \log n$, where n is the BO. For more details, see the Supporting Information.

(73) The SSF^+ cation claimed to be present as its BF_4^- and AsF_6^- salts on the basis of IR spectroscopy would possess an even shorter S−S bond with a higher bond order (Seel, F.; Hartmann, V.; Molnar, I.; Budenz, R.; Gombler, W. *Angew. Chem.* **1971**, *83*, 173; *Angew. Chem., Int. Ed. Engl.* **1971**, *10*, 186.). The calculated (PBE0/cc-pVTZ) S−S bond length of 1.823 Å corresponds to a bond order of about 2.5.